Burkholderia vietnamiensis Genes Involved in Extracellular Medium-Chain-Length Polyhydroxyalkanoate Degradation

Running title: Extracellular PHA Degradation Genes in *Burkholderia vietnamiensis*

Zhong Ling Yap[a], Sion Yi[a], Ernesto Quintana[a], Gabriel G. Lucas[b], Mohamad Safklou[a], Ryan Darragh[a], Andrew M. Hogan[a], Anna Motnenko[a], Warren Blunt[c], Richard Sparling[a], Dario Fernández Do Porto[b], David B. Levin[c], Silvia T. Cardona[a,d*]

Department of Microbiology, University of Manitoba, Winnipeg, Manitoba, Canada R3T 2N2

[b]Plataforma de Bioinformática Argentina, Instituto de Cálculo, Ciudad Universitaria, Facultad de Ciencias Exactas y Naturales, Universidad de Buenos Aires (UBA), Ciudad Autónoma de Buenos Aires, Argentina

[c]Department of Biosystems Engineering, University of Manitoba, Winnipeg, Manitoba, Canada R3T 5V6

[d]Department of Medical Microbiology and Infectious Diseases, University of Manitoba, Winnipeg, Manitoba, Canada R3E 0J9

email: silvia.cardona@umanitoba.ca

Keywords: *Burkholderia*, *Burkholderia vietnamiensis*, Transposon mutagenesis, RhaCAST, gene insertion, Tn-seq

Abstract

Bioplastics represent promising alternatives to petroleum-based plastics, yet their biodegradation remains insufficiently understood. Identifying bacteria capable of degrading bioplastics extracellularly could enhance end-of-life management practices. To investigate *Burkholderia*'s capacities for the degradation of medium-chain-length polyhydroxyalkanoate (mcl-PHA), we screened a panel of *Burkholderia* strains and identified such capacity in strains of *B. gladioli*, *B. multivorans,* and *B. vietnamiensis*. To elucidate the genetic basis of this activity, we performed transposon mutagenesis followed by activity-based screening and Tn-seq on *B. vietnamiensis* LMG 16232. Disrupted genetic elements in transposon mutants with negative phenotypes were further investigated using a CRISPR-associated transposase (CAST) system. These included a lipase production gene cluster, encoding two putative triacylglycerol lipases and a chaperone, and genes coding for a a A24 family peptidase, a TetR/AcrR family transcriptional regulator and a type II secretion system (T2SS) protein. Complete loss or reduced extracellular mcl-PHA depolymerase activity was observed in the CAST mutants, validating their involvement in mcl-PHA degradation. Notably, only one of the two lipases encoded in the lipase production gene cluster was responsible for mcl-PHA degradation, suggesting that while lipases may show substrate promiscuity, lipase functional annotation does not necessarily imply mcl-PHA depolymerization. Docking experiments using the amino acid sequences of the two lipases supported these findings. Together, we identify a gene coding for an active mcl-PHA depolymerase in *B. vietnamiensis* and demonstrate the power of combining activity-based screening, Tn-seq, and CAST to rapidly establish gene-to-function links.

42 **Importance**

43 Due to their versatile metabolism, *Burkholderia* strains play critical roles in degradation of multiple
44 compounds in the environment. Here we show that several *Burkholderia* species can extracellularly degrade
45 medium-chain-length polyhydroxyalkanoates (mcl-PHAs), a promising class of bioplastics. By integrating
46 transposon mutagenesis, Tn-seq, and CRISPR-associated transposase (CAST) technologies, we identify
47 and validate key genetic determinants involved in mcl-PHA degradation in *B. vietnamiensis*. These genes
48 encode a lipase, a secretion system component, and regulatory factors, underscoring the complexity and
49 specificity of microbial bioplastic degradation pathways. These findings not only advance our
50 understanding of PHA biodegradation but also identifies *B. vietnamiensis* as as a source of enzymes capable
51 of degrading extracellular mcl-PHA.

52

53

54 **Introduction**

55 Environmental pollution from petroleum-based plastic has driven growing interest in
56 bioplastics, which are bio-based, biodegradable substitutes. Among these, poly(3-
57 hydroxyalkanoates) (PHAs) are microbially produced polyesters that have a wide-range of
58 applications in various sectors, such as packaging, agriculture, and biomedical devices (1). PHAs
59 are synthesized by many microorganisms for intracellular energy and carbon storage under
60 conditions of nutrient imbalance, namely nitrogen and phosphorus limitation. Depending on the
61 number of carbon atoms in each 3-hydroxyalkanoate monomer unit, PHAs can be broadly
62 classified as either short-chain-length PHAs (scl-PHA), which consist of 3–5 carbons per monomer
63 or medium-chain-length PHAs (mcl-PHA), which contain, 6–14 carbons per monomer, each with
64 different physico-chemical properties (2). The carbon side chain length of each monomer will
65 influence the enzyme-substrate specificity for degradation (3).

66 PHAs are degraded by either intracellular or extracellular PHA depolymerases.
67 Intracellular PHA depolymerases hydrolyze PHA or carbonosomes, which are intracellular carbon
68 reservoirs that can contain PHA granules (4). Extracellular PHA depolymerases degrade
69 exogenous denatured granules that are semi-crystalline and lack the surface layer (3). Both
70 intracellular and extracellular PHA depolymerases are carboxylesterases and belong to the α/β-
71 hydrolase fold family (5). PHA depolymerases have been isolated and biochemically characterized
72 in Firmicutes, Proteobacteria, Actinobacteria, and Ascomycete fungi (6).

73 Many studies have reported microorganisms that degrade scl-PHA, and have purified and
74 characterized the corresponding enzymes (5, 6). However, microorganisms that can degrade mcl-
75 PHA are relatively rare compared to those that can degrade scl-PHA (6). Most of the extracellular
76 mcl-PHA depolymerases that have been purified and biochemically validated belong to

77 *Pseudomonas* species (7–9), the obligate predator *Bdellovibrio bacteriovorus* (10), *Thermus*
78 *thermophilus* (11) and *Streptomyces* species (12–14). Amino acid sequence similarity searches of
79 metagenomes using biochemically validated extracellular mcl-PHA depolymerases as queries,
80 have identified candidate extracellular mcl-PHA depolymerases only in the taxonomic groups
81 Myxococcota, Proteobacteria, Actinobacteriota and Bdellovibrionota (6). These studies suggest
82 that mcl-PHA degradation is not widely distributed among Bacteria.

83 While all extracellular PHA depolymerases hydrolyze PHA, extracellular mcl-PHA
84 depolymerases show little overall sequence homology with scl-PHA. However, PHA
85 depolymerases share structural and mechanistic characteristics with lipases and other α/β-
86 hydrolase enzymes (15). Both PHA depolymerases and lipases have a GxSxG sequence motif
87 found in other α/β-hydrolases and known as the lipase box and a catalytic triad consisting of the
88 central serine of the lipase box, histidine and aspartic acid (16), underscoring a not fully-
89 understood functional promiscuity between PHA depolymerases and lipases. Indeed, some
90 extracellular lipases purified from various species, including *Bacillus subtilis, Pseudomonas*
91 *aeruginosa, Pseudomonas alcaligenes,* and *Pseudomonas fluorescens* (16) were not able to
92 hydrolyze poly3-hydroxyhexanoate or poly3-hydroxybutyrate. However, the extracellular lipases
93 of *Pseudomonas chlororaphis* PA23 and *Acinetobacter lwoffii* can hydrolyze various PHA
94 polymers, including the mcl-PHA polyhydroxyoctanoate (PHO) and polyhydroxydecanoate (17).
95 While *Burkholderia* strains are known lipase producers (18–21) and the structure of a *B. cepacia*
96 lipase has extensively described (22–26), the capacity to degrade extracellular mcl-PHA in the
97 *Burkholderia* genus has not been investigated.

98 In this work, we investigated mcl-PHA degradation capacities in *Burkholderia* using PHO
99 as a model substrate. By combining activity-based screening with the power of random and site-

100 directed transposon mutagenesis, we were able to rapidly identify genetic elements that contribute
101 to mcl-PHA degradation in *B. vietnamiensis* LMG 16232. Specifically, we identified the loci
102 P4G95_16805 and P4G95_16810 encoding lipases but only PG95_16805 (*lip1*) is responsible for
103 PHO degradation, while P4G95 1680 (*lip2*) is not. The distinct activities would not have been
104 predicted based on gene annotation alone.
105

106 **Results**

107 *Diversity of extracellular mcl-PHA degradation activity in Burkholderia strains*

108 To identify mcl-PHA degradation activity in the *Burkholderia* genus, we performed an
109 initial screen in a solid minimal medium containing PHO and limiting amounts of phenylalanine,
110 supplemented with Nile red to enhance the visualization of PHO degradation as a clear halo around
111 isolated bacterial colonies. Phenylalanine was chosen as a secondary carbon source in the medium
112 because: i) it is known to be catabolized by *Burkholderia* species (27), and ii) its metabolism is
113 known to influence several bacterial pathways (28). The plates were incubated for 20 days to
114 ensure cells grew densely and produced sufficient enzyme to visually detect mcl-PHA degradation.
115 After dense growth was achieved, a clear halo was observed around some colonies, suggesting
116 extracellular PHO degradation.

117 Several strains of *B. gladioli*, *B. multivorans*, and *B. vietnamiensis,* were able to produce a
118 visible halo suggesting extracellular mcl-PHA degradation (**Table 1, Fig. S1**). While *B. stagnalis*
119 strains MSMB618, MSMB642, and *B. vietnamiensis* LMG 16232 had moderate activity, *B.*
120 *gladioli* strain VC19233, *B. multivorans* 21NH942533, and VC9825 exhibited weaker activity in
121 degrading mcl-PHA. Two strains, *B. multivorans* F9091687 and *B. gladioli* 132208 observed

122 temperature-dependent mcl-PHA degradation activity. No activity was observed for *B.*
123 *cenocepacia*, *B. contaminans,* and *B. dolosa* isolates tested (**Table 1**).

124 *Genetic basis of B. vietnamiensis LMG 16232 extracellular mcl-PHA degradation activity*

125 To determine the genetic elements involved in extracellular mcl-PHA degradation activity,
126 we selected *B. vietnamiensis* LMG 16232 (29) for transposon mutagenesis and activity-based
127 screening followed by identification of transposon sites with Illumina sequencing (Tn-seq) (**Fig.**
128 **1**). To achieve genomic coverage of transposon insertions in *B. vietnamiensis* LMG 16232, we
129 determined the estimated transposon insertion density using an analytical model based on a
130 Poisson distribution of transposon insertions (30) (see Materials and Methods).

131 The primary screening of single isolated transconjugants identified 84 colonies that did not
132 produce the visible halo associated with mcl-PHA degradation. These colonies were subjected to
133 secondary screening, where each isolated transconjugant clone was propagated and screened on
134 solid medium containing mcl-PHA. We observed that 66 transconjugants had lost the ability to
135 degrade extracellular mcl-PHA, showing no halo (pool 1). In contrast, 18 transconjugants
136 exhibited a reduced halo (pool 2). Enrichment of transposon insertions followed by Illumina
137 sequencing identified several disrupted genetic elements. Pool 1 and pool 2 contained transposon
138 mutants with insertions in 18 and 12 unique loci, respectively (Table 2).

139 Further examination of the transposon insertions identified gene clusters (P4G95_05485,
140 P4G95_05490, P4G95_05495, P4G95_05500, P4G95_05505, P4G95_05510, P4G95_05515,
141 P4G95_05520, P4G95_05525, P4G95_05530, P4G95_05535) encoding a T2SS (**Fig. 2A**), and a
142 lipase gene cluster, encoding two triacylglycerol lipases and a lipase chaperone (P4G95_16805,
143 P4G16810 and P4G16815, respectively (named *lip1*, *lip2* and l*ipO* herein) (**Fig. 2B**). While
144 activity-abolishing insertions were identified in *lip1* and *lipO*, no transposon insertions that

145 resulted in loss of mcl-PHA degradation were identified in the *lip2* gene, suggesting that *lip1*
146 (P4G95_16805) but not *lip2* (P4G95_16810) might be responsible for extracellular mcl-PHA
147 degradation.

148 Another identified gene cluster was related to the biosynthesis of polyhydroxybutyrate.
149 Transposon insertion sites in this cluster were found in *phaR* (P4G95_13560), a PHA synthesis
150 repressor and *phaA* (P4G95_13570), which encodes for an acetyl-CoA acetyltransferase involved
151 in the biosynthesis of polyhydroxybutyrate (**Fig. 2C**). In addition, a gene coding for a A24 family
152 peptidase (P4G95_07805) and four genes encoding transcriptional regulators were identified,
153 which are a TetR/AcrR family transcriptional regulator (P4G95_00865), a MarR family winged
154 helix-turn-helix transcriptional regulator CDS (P4G95_05570), *phaR* (P4G95_13560), the
155 polyhydroxyalkanoate synthesis repressor, and a helix-turn-helix domain-containing protein CDS
156 (P4G95_16325) (Table 2). Together, the identified genetic elements suggest the Lip1 lipase, which
157 contains a signal peptide, is cleaved by the A24 family peptidase (P4G95_07805) and is assisted
158 by the LipO lipase chaperone for folding and activation prior to secretion via the T2SS. Finally,
159 the regulatory elements identified together with the *pha* gene cluster suggest that activation of mcl-
160 PHA degradation is regulated and intertwined with PHA biosynthesis.

161 A few genetic elements obtained from the Tn-seq analysis had a less clear relation with
162 extracellular mcl-PHA degradation in *B. vietnamiensis* LMG 16232. These were genes encoding
163 for trehalose-6-phosphate phosphatase (P4G95_10885), hypothetical proteins (P4G95_20805 and
164 P4G95_20810), the N-acetylglucosamine-6-phosphate deacetylase, NagA (P4G95_03530), a
165 phenylacetate-CoA oxygenase/reductase subunit PaaK and PaaJ (P4G95_06510 and
166 P4G95_06515) and an acetyl-CoA acetyltransferase PhaA (P4G95_13570).

167 *Genetic elements responsible for mcl-PHA degradation are confirmed by RhaCAST*

168 To validate the genetic elements involved in extracellular mcl-PHA degradation activity identified
169 by Tn-seq, we created independent insertional mutants with our previously developed RhaCAST
170 system (31), which uses a rhamnose-inducible CRISPR-associated transposase (CAST)-based
171 delivery of transposons (32) for targeted insertional mutagenesis in target genes. We applied
172 RhaCAST in *B. vietnamiensis* LMG 16232 (**Fig. 3A**) interrupting genes previously detected by
173 our Tn-seq approach. We successfully produced insertional mutants for genes encoding the
174 putative lipase (*lip1*, P4G95_16805), the A24 family peptidase (*A24*, P4G95_07805), the
175 TetR/AcrR family transcriptional regulator (*tetR/acrR*, P4G95_00865), trehalose-phosphatase
176 (*otsB,* P4G95_10885), and a T2SS protein (*gspE*, P4G95_05530) (**Fig. S2-6**). Inoculation and
177 growth of these mutants on agar plates containing mcl-PHA failed to produce a WT-like visible
178 halo around the colonies (**Fig. 3B**), confirming the link between the interrupted genetic elements
179 and the observed phenotype. To further confirm that the halo of degradation observed corresponds
180 to mcl-PHA degradation, plugs of agar from underneath WT and *lip1* mutant growth were taken
181 and the presence of PHO in the agar was assessed with by gas chromatography with flame
182 ionization detection (GC-FID). As expected, no PHO was detected in the agar beneath the WT
183 strain, whereas PHO was detected under the *lip1* strain, indicating that PHO was not being
184 degraded (**Fig. 4**). We note that after many attempts, we were unsuccessful in producing a
185 RhaCAST *lipO* mutant for unknown reasons.

186 *Phenotypic and gene expression analysis of the lipase production gene cluster confirms that lip1,*
187 *but not lip2, is responsible for extracellular mcl-PHA degradation*

188 High-density transposon mutagenesis followed by Tn-seq analysis uncovered the
189 involvement of a lipase production gene cluster (**Fig. 2B** and **Fig. 5A**). From this analysis, colonies
190 with no halo were found to have insertions in *lip1* and *lipO* (**Fig. 5B**) but transposon insertions in

191 *lip2* were not found when sequencing the halo-defective colonies (**Fig. 5B**, N.D). This finding was
192 intriguing for two reasons; first, it seemed that Lip2 had no enzymatic activity against mcl-PHA,
193 despite displaying 78% identity and 86% similarity to Lip1 (**Fig. S7**). Second, as *lip2* and *lipO*
194 seem to be organized in an operon, one might expect that transposon interruptions in *lip2* would
195 result in a halo-defective phenotype because transposon insertions in *lipO* produced no halo around
196 the colonies (**Fig. 5B**). To further elucidate these conflicting results, we used RhaCAST to
197 construct a *lip2* mutant (**Fig. 5B, Fig. S8**). The *lip2* mutant displayed a WT-like halo, indicating
198 mcl-PHA degradation (**Fig. 5B**) and supporting the involvement of only *lip1* in mcl-PHA
199 degradation activity. Furthermore, gene expression analysis of the *lip2* mutant by RT-PCR
200 demonstrated that *lipO* was expressed ruling out a polar effect of the RhaCAST system on this
201 putative operon (**Fig. 5C**). The *lipO* gene was also expressed in the *lip1* mutant (**Fig. 5D**).

202 As Lip2 was not involved in extracellular mcl-PHA degradation, we compared the activity
203 of *lip1* and *lip2* mutants towards tributyrin, a well-known substrate for lipase activity (33) and
204 quantified degradation halos of biological replicates (**Fig. 6**). The wild-type *B. vietnamiensis* LMG
205 16232 exhibited consistent activity against mcl-PHA (**Fig. 6A**). Instead, the *lip1* mutant exhibited
206 no activity against mcl-PHA, confirming its role as solely responsible for mcl-PHA degradation.
207 *B. vietnamiensis* LMG 16232 WT also degraded tributyrin (**Fig. 6B**). However, the tributyrin
208 degrading activity of the *lip1* mutant was only reduced but not abolished (**Fig. 6B**), suggesting that
209 other lipases, including *lip2,* might be active lipases. mcl-PHA and tributyrin degradation were
210 also not affected in the *lip2* mutant (**Fig. 6A and B**). In summary, while Lip1 appears to be active
211 against extracellular mcl-PHA and tributyrin, Lip2 may be active against tributyrin but not against
212 mcl-PHA.

Structural analysis of Lip1 and Lip2 putative amino acid sequences reveal differences in the catalytic site.

To further investigate the differential activity of Lip1 and Lip2, we first compared their sequences with the well characterized *B. cepacia* lipase (22, 24) and experimentally validated mcl-PHA depolymerases from *Streptomyces roseolus* and *S. venezuelae*, (13, 14) and *Pseudomonas* (7–9), as well as *Bdellovibrio* (10). The multiple alignment (**Fig. S9**) revealed that Lip1 and Lip2 showed high similarity to the *B. cepacia* lipase (97.8% and 93.9%, respectively). Instead, less than 30% similarity was found between Lip1 or Lip2 to any of the other mcl-PHA depolymerases beyond the presence of the conserved lipase box. We then predicted the structures of Lip1 and Lip2 using AlphaFold 2 and assessed multiple sequence alignments. The sequence coverage analysis, which combines alignment depth and sequence identity, illustrates the extent of conservation across homologous sequences for both proteins (**Fig. S10A**). A well-conserved core region (residues ~50–160) is evident in both cases, with lower coverage and diversity in the N- and C-terminal regions suggesting flexible or functionally variable domains. Consistent patterns in Predicted Aligned Error (PAE) matrices of the five top-ranked models support a robust domain architecture with potential inter-domain flexibility (**Fig. S10B**). Additionally, the high predicted Local Distance Difference Test (pLDDT) scores (**Fig. S10C**) further validate the confidence in structural predictions. The high pLDDT values (>90) in the core region confirm a well-defined fold, whereas significant drops around residues 50–100 and 200–250 suggest intrinsically disordered or flexible regions. These trends are consistent across both Lip1 and Lip2, reinforcing the reliability of the predictions and indicating a shared structural organization.

Superposition of the AlphaFold-predicted Lip1 structure (**Fig. S11**) with the *B. cepacia* lipase (PDB ID 4LIP**)** crystallographic template revealed a high degree of structural similarity except for

236 an alpha-helix, which appears to obstruct a cavity present in 4LIP. To evaluate the catalytic sites
237 in the context of the observed *lip1* and *lip2* mutant phenotypes, we performed a structural
238 superposition with the *B. cepacia* lipase. The overlay reveals a remarkable similarity in the spatial
239 arrangement of the catalytic triad (**Fig. S12**). The conserved positioning of the key catalytic
240 residues strongly suggests that Lip1 and Lip2 adopt a functional fold compatible with lipase
241 activity. This structural conservation provides additional support for the hypothesis that both
242 proteins share mechanistic features with known lipases.

243 Using the *B. cepacia* lipase as a template, we guided the docking of Lip1 and Lip2 with
244 two substrates: 3-Hydroxyoctanoate (OCT) and Tributyrin (TRI). Both ligands were energy-
245 minimized before docking, and a grid-based docking algorithm was used to position the ligands
246 within the predicted active sites of both proteins. Notably, all combinations of protein-ligand
247 docking yielded clusters with low energy, indicating favourable interactions (**Table S1**).

248 Docking simulations with Lip1 revealed a single predominant low-energy cluster for both
249 OCT and TRI (**Fig. 7A, B, E, Table S1**). This convergence, together with the consistently low
250 binding energies, strongly suggests a high affinity between Lip1 and both ligands. In contrast, the
251 docking of both ligands against Lip2 (**Fig. 7C, D, E, Table S1**) yielded three distinct low-energy
252 clusters for each substrate. This multiplicity of binding modes suggests a weaker or less specific
253 interaction, potentially due to a more flexible or heterogeneous binding pocket that compromises
254 optimal substrate accommodation. Structural analysis of the catalytic site revealed that Lip1 and
255 the *B. cepacia* lipase share a similar configuration, whereas Lip2 contains a different amino acid
256 at position 73 compared to Lip1, which is glutamine (Lip2) instead of tyrosine (Lip1) (**Fig. S7,**
257 **Fig. 7F**). This amino acid difference may explain the different phenotypes of the *lip1* and *lip2*
258 mutants in which activity against mcl-PHO was only observed in the *lip2* (but not l*ip1*) mutant.

259 **Discussion**

260 The production and use of bioplastics, including mcl-PHA, have increased recently. These
261 materials are considered alternatives to petroleum-based plastics because they can be derived from
262 renewable resources and have a wide range of applications (1). Despite growing interest,
263 microorganisms and enzymes capable of degrading mcl-PHA remain relatively understudied (6).
264 Extracellular mcl-PHA depolymerases have been found in some genera, including *Pseudomonas*
265 (7–9), *Bdellovibrio* (10), *Thermus* (11) and *Streptomyces* (12–14). However, to date, the
266 mechanism of action for extracellular mcl-PHA by microorganisms has not been thoroughly
267 explored. Here, we report that several *Burkholderia* strains, including *B. gladioli*, *B. multivorans*,
268 and *B. vietnamiensis,* can degrade mcl-PHA. Through transposon mutagenesis combined with Tn-
269 seq analysis, we identified genetic elements associated with mcl-PHA degradation in *B.*
270 *vietnamiensis* LMG 16232. We further validated some of these genetic elements by generating
271 targeted insertional mutants using RhaCAST and tested their extracellular mcl-PHA degradation
272 activity. Our findings indicate that the enzyme responsible for extracellular mcl-PHA degradation
273 is a lipase (Lip1) with substrate versatility and we ruled out the involvement of a second lipase
274 (Lip2) encoded downstream of *lip1*. Indeed, the *lip2* mutant constructed with our RhaCAST
275 system, had similar extracellular mcl-PHA activity compared to the wild type. Therefore, we show
276 experimental evidence of *Burkholderia*'s capability to degrade extracellular mcl-PHA, linking the
277 enzymatic activity to the P4G95_16805 locus (*lip1*) of *B. vietnamiensis* LMG 16232, and ruling out
278 the involvement of *lip2* (P4G95_16810).

279 A technique commonly used to enhance the visualization of PHA degradation involves
280 incorporating Nile red, a lipophilic fluorescent dye, into agar plates (34). Thus, we adopted this
281 visualization method in our screening medium to increase sensitivity. In comparison to other

282 studies, where the degradation of extracellular mcl-PHA can be observed within 2 to 3 days,
283 *Burkholderia vietnamiensis* LMG16232 exhibited a slower degradation process, requiring
284 approximately 7 days for observable activity, suggesting co-metabolism, and/or poor growth on
285 mcl-PHA. Some strains of *Burkholderia* from the initial screening showed weak activity, with
286 degradation taking up to 20 days, despite the use of Nile red to enhance detection. Nevertheless,
287 by implementing this visualization technique alongside transposon mutagenesis in *B.*
288 *vietnamiensis* LMG 16232, we were able to screen 50,000 individual colonies in a rapid manner.
289 This approach enabled us to identify transconjugant colonies that had lost the ability to degrade
290 mcl-PHA, providing a sensitive and efficient screening method. This method may be applicable to
291 other polymers that can be stained with suitable dyes, enhancing assay sensitivity.

292 Besides the identification of *lip1* as the gene encoding an enzyme capable of mcl-PHA
293 degradation, transposon mutagenesis combined with Tn-seq identified other genetic elements
294 involved in the degradation of mcl-PHA in *B. vietnamiensis* LMG 16232 (**Fig. 8**). These genes can
295 be classified into three functional groups: a) lipase/chaperone gene cluster, b) components of
296 T2SS, and c) regulatory elements. The genetic elements associated with the mcl-PHA degradation
297 in *B. vietnamiensis* LMG 16232 are consistent with the findings in various *Burkholderia* lipases,
298 particularly regarding the production, chaperone-assisted folding and secretion of extracellular
299 lipases by T2SSs (35, 36). Similar to the lipases from other *Burkholderia* species, the identified *B.*
300 *vietnamiensis* LMG 16232 LipO is expected to assist the correct folding and efficient secretion of
301 Lip1 via the T2SS. Many *Burkholderia* strains can secrete extracellular lipases under inducing
302 conditions, and some of those lipases are capable of degrading various compounds (37–40). For
303 example, lipases from *Burkholderia* stains MC 16-3 (GenBank: AY772173) and 99-2-1
304 (GenBank: AY772174) can degrade methyl(R)-N-(2,6-dimethyl-phenyl)alaninate (41).

305 Additionally, the lipase from *B. cepacia* PBSA-1 (GenBank: EF189714.1) has been shown to
306 degrade poly(butylene succinate-co-butylene adipate) (42), while *B. cepacia* lipase can degrade
307 polycaprolactone (PCL) (16). These lipases, including the ones identified in this work, share the
308 conserved lipase box of G-H-S-Q-G. While *B. cepacia* DP1 is a major lipase producer and has
309 been shown to degrade extracellular scl-PHA (43, 44), there was no report of *Burkholderia* species
310 that degrade extracellular mcl-PHA.

311 One of the putative regulatory elements identified in this work is a TetR/AcrR family
312 transcriptional regulator CDS (P4G95_00865). This type of regulator is widely distributed among
313 bacteria and controls various cellular processes, including the metabolism of lipid compounds,
314 such as the synthesis and degradation of fatty acid and the storage of polymer (45). The
315 involvement of other regulatory elements, such as HTH-type transcriptional activators and a PHA
316 synthesis repressor, suggests that extracellular mcl-PHA degradation activity of *B. vietnamiensis*
317 LMG 16232 may be integrated with other metabolic pathways. While we did not identify a specific
318 genetic element directly responsible for the uptake of mcl-PHA degradation products, we propose
319 passive diffusion. This hypothesis is based on the structural similarity between mcl-PHA
320 monomers and fatty acids, which both contain a hydrophobic alkyl chain (46). Medium-chain fatty
321 acids (C_7-C_{11}) can enter bacteria through simple diffusion without the involvement of active
322 transport systems or an unknown mechanism (47, 48).

323 Enzymes that degrade extracellular mcl-PHA and lipases exhibit similar characteristics,
324 including the presence of the lipase box and a conserved non-catalytic amino acid triad (16).
325 Consequently, this study suggests that the mcl-PHA degrading enzyme from *Burkholderia* are
326 lipases that may also possess the capability to degrade mcl-PHA. However, Lip2 (P4G95_16810)
327 is annotated as a lipase, contains the lipase box and is highly similar to Lip1, yet our experimental

328 evidence indicates this lipase cannot degrade mcl-PHA. Our structural analysis of Lip1 and Lip2,
329 based on AlphaFold predictions, highlights a conserved core architecture and variable N- and C-
330 terminal regions, suggesting potential regulatory or accessory roles. Superposition with the *B.*
331 *cepacia* lipase PDB structure 4LIP demonstrated overall structural similarity but also revealed an
332 obstructive alpha-helix in Lip1 and Lip2, which is absent in 4LIP, and may influence enzyme
333 activity. While both Lip1 and Lip2 maintain a conserved catalytic triad, consistent with lipase
334 activity, docking experiments with ligands tributyrin and octanoate showed strong and specific
335 binding for Lip1. In contrast, Lip2 exhibited multiple binding modes, indicating a more flexible
336 binding pocket. A difference in the amino acid at position 73: (Lip1 contains glutamine, while
337 Lip2 has tyrosine) is suggestive of differential catalytic activity.

338 In summary, Lip1 appears to function as an active lipase and mcl-PHA depolymerase, while Lip2
339 may have altered activity due to structural differences. Additional biochemical and structural
340 studies will be needed to validate these conclusions. Overall, this study demonstrates the power of
341 visual screens combined with high-density transposon mutagenesis to establish gene-to-function
342 links and provides new insight onto the degradation of extracellular mcl-PHA by the genus
343 *Burkholderia*.

344 **Material and methods**

345 *Strains, Selective Antibiotics, and Growth Conditions*

346 Strains and plasmids are shown in **Table 3**. Primers used in this study are listed in **Table**
347 **4**. All strains were grown in LB-Lennox medium (Difco). Strains of *Burkholderia* and the strains
348 of *E. coli* were initially grown at 37 °C, except for *E. coli* Stbl2, which was grown at 30 °C. The
349 following selective antibiotics were used: chloramphenicol (Sigma; 20 µg/mL for *E. coli*),

350 trimethoprim (Sigma; 100 µg/mL for strains of *Burkholderia*, 50 µg/mL for *E. coli*), gentamicin
351 (Sigma; 50 µg/mL for *Burkholderia*).

352 *Genomic and plasmid extraction*

353 Genomic DNA of the *B. vietnamiensis* LMG 16232 mutants made with RhaCAST were
354 extracted using the PureLink microbiome DNA purification kit (Invitrogen). Genomic DNA of the
355 Tn-seq pools were extracted using standard isopropanol precipitation (49). Plasmid DNA was
356 extracted using the EZNA Plasmid DNA Mini Kit (Omega Bio-tek). Both genomic and plasmid
357 DNA were eluted or solubilized in Tris-HCl pH 8.5.

358 *Substrate and media preparation*

359 The poly(3-hydroxyoctanoate) (PHO) (Product name: VersaMer-8-90) colloidal
360 suspension was created by dissolving 400 mg of PHO (Polyferm Canada Inc., Canada) into 200
361 mL acetone. Once the PHO was dissolved, 40 mL of dH_2O was added. The acetone was evaporated
362 off using a speed evaporator. The colloidal suspension was stored at 4˚ C until needed.

363 The mcl-PHA containing medium consisted of an M9 minimal medium agar (BD Difco,
364 USA) with 2 mM phenylalanine, 2 mM $MgSO_4$, 10 mg/ mL of PHO and 0.3 µg/mL Nile red. PHO
365 was added to the medium by using a previously prepared colloidal suspension of PHO. The PHO,
366 Nile red, $MgSO_4$, and phenylalanine were added after autoclaving to melted M9 agar. 25 mL of
367 medium was then poured into petri plates. After solidifying, the plates were stored at 4°C until
368 needed.

369 Tributyrin medium was made using a minimal medium with 2 mM phenylalanine and 2
370 mM $MgSO_4$ with tributyrin added to a final concentration of 4% (v/v) to the medium according to
371 the Sigma-Aldrich instructions (Sigma, St. Louis, Missouri, USA). The tributyrin was added after

372 autoclaving whilst the agar medium was around 80°C. The medium with tributyrin was vigorously
373 mixed until ready to pour into petri plates. After solidifying, the plates were stored at 4°C until
374 needed.

375 *Screening for mcl-PHA and tributyrin degradation*

376 To determine the strain's ability to degrade mcl-PHA and tributyrin degradation. The
377 overnight cultures were grown at 30°C and washed twice with PBS. 20 μL of the culture was
378 inoculated after being adjusted to an OD_{600} of 1. For mcl-PHA degradation determination, the
379 plates were incubated for 7-20 days; For tributyrin degradation determination, the plates were
380 incubated for 3 days, both incubated at 30°C. The visualization of the halo degradation was
381 performed using AlphaImager EP (Cell Biosciences, Santa Clara, CA). For the mcl-PHA plates
382 containing Nile red, the image was taken under UV excitation. Colonies that appeared to have lost
383 the PHO degradation activity on the first round of screening were then subjected to a secondary
384 screening to rule out false positives. 66 and 18 transconjugants were isolated without or with weak
385 PHO degradation activity, respectively.

386 *Transposon mutagenesis, Tn-seq library preparation and genome mapping*

387 *B. vietnamiensis* LMG 16232 was subjected to transposon mutagenesis with
388 pRBrhaBoutgfp (50). A total of 50,000 single colonies were screened. This number is based on
389 the expected average transposon insertion density from the model, approximately eight transposon
390 insertions per gene. Assuming a genome with N = 6000 non-essential genes and a collection of N
391 = 50,000 transposon insertion mutants, the probability that a single gene will see no transposon
392 insertions is: P(0, k, N) = e^(-50,000/6,000) = 2.4×10^{-4}; the total number of genes that will see no
393 insertions is: N* e^(-k/N) = 6,000 x 2.4×10^{-4} = 1.4 genes; and the total number of genes will be
394 found with this transposon density is n(insertion) 6,000* (1-e ^(-50,000/ 6,000)) = 5,999 genes.

395 Tn-seq was chosen to identify the transposon insertion sites. To enrich transposon-genome
396 junctions and to determine the insertion site, an adapted Tn-seq method, Tn-seq circle, developed
397 by Gallagher et al. (51), was performed as previously described with some minor modifications
398 (49, 51). Briefly, cultures of individual mutants were grown individually to approximately OD_{600}
399 of 3 and were combined into two separate pools, based on without (Pool 1) or with weak (Pool 2)
400 PHO degradation activity. The cultures were harvested, followed by the genomic DNA extraction.
401 The DNA was sheared to an average size of 300 bp via ultrasonication with a Covaris M220 (duty
402 factor of 20%, a peak incident power of 50W, 200 cycles per burst, and a duration of 75s), followed
403 by end repair with the NEBNext End Repair Module (NEB) and A-tailing. Next, the products were
404 ligated with adaptors, consisting of annealing oligos 683 and 684 with the Quick Ligation Kit
405 (NEB) and digested with *PacI* (NEB). Probe 682 in the presence of Ampligase (Lucigen) was used
406 to circularize fragments containing the transposon sequence. The exonuclease treatment was
407 carried out with a mix of T7 gene 6 exonuclease (ThermoFisher), Lambda exonuclease (NEB),
408 and Exonuclease I (NEB) to digest the linear fragments. The enrichment of the transposon–genome
409 junctions was confirmed by comparing the amplification of the transconjugant's pools with wild-
410 type *B. vietnamiensis* LMG 16232 using qPCR with iTaq Universal SYBR Green Supermix (Bio-
411 Rad). The number of PCR cycles corresponding to ~50% saturation by qPCR was chosen to
412 amplify transposon-genome junctions with iTaq DNA polymerases (Bio-Rad) for Illumina
413 sequencing. PCR primers 681, 690, 718, and 719 contain the Nextera indices and were used in
414 appropriate pairs (**Table 4**). The indexed samples were then cleaned up with SeraMag beads
415 (Cytiva), analysed on a TapeStation4150 (Agilent Technologies) and sequenced with an Illumina
416 MiSeq 2500. Raw reads were deposited in the NCBI Sequence Read Archive (SRA) repository

417 and will be publicly available after publication under BioProject: PRJNA1082765, accession:
418 SRR28216496 (Pool 1), SRR28216495 (Pool 2).

419 The sequenced reads of these mutants were mapped to the *B. vietnamiensis* LMG 16232
420 genome with the Galaxy bioinformatics platform (https://usegalaxy.org). Using Cutadapt
421 (Galaxy v2.9+galaxy0) (52), the transposon sequence
422 5'-NNNNAATCTAGACTAGTGCGGCCGCACTTGTGTATAAGAGTCA-3' was removed
423 from the FASTQ file. Next, using Burrows-Wheeler transform (BWA) (Galaxy v0.7.17.4) (53),
424 the reads were mapped to the close genome of *B. vietnamiensis* LMG 16232 (29). The BWA's
425 BAM output was then converted to SAM using BAM-to-SAM (Galaxy 2.0.2) (54). The output
426 was visualized using Geneious 8.1.9.

427 *Determination of the PHO content beneath inoculated culture*

428 After 4 days, the bacterial growth from the inoculated culture from the phenotypic assay
429 was scraped off from the agar. An agar disk beneath the inoculated culture was cut using the back
430 of the P1000 pipette tip. For control, a disk was cut where no cell was inoculated. The samples
431 were dried at 60°C for 16 hours, and the PHO was extracted in chloroform using the acid-catalyzed
432 methanolysis procedure as previously described (55, 56). The determination of PHO in the agar
433 was performed using an Agilent 7890A gas chromatograph equipped with a DB-23 capillary
434 column (30 m × 250 µm × 0.25 µm) and a flame ionization detector (Agilent Technologies, Santa
435 Clara, CA). Method operating parameters and peak quantification have been previously described
436 (55, 57). The retention times and response factors for methyl 3-hydroxyoctanic acid were
437 confirmed using standards purchased from Cayman Chemical (Catalogue # 24609).

438 *Gene expression analysis by reverse transcriptase (RT)PCR*

439 To determine the effect of RhaCAST insertion in *lip1* and *lip2* on the expression of
440 downstream genes, RT-PCR was performed. Briefly, *B. vietnamiensi*s LMG 16232 Wildtype, *lip1*,
441 and *lip2* mutants were grown overnight on LB media at 30°C, the cultures were washed twice with
442 PBS and adjusted to OD_{600} of 1 (Time 0). Twenty µL of the adjusted cultures were then plated
443 onto PHO plates. Bacterial growth was harvested from the plates at days 4 and 7 and the RNA was
444 extracted following PureLink RNA Mini Kit protocol (Invitrogen™) following the manufacture's
445 instructions for bacterial cells. The RNA was then converted to cDNA using a SuperScript IV
446 VILO Master Mix Kit (ThermoFisher). The PCR reactions were performed with the Q5 High-
447 Fidelity DNA polymerase (New England Biolabs) following the manufacturer's instructions.

448 *In silico analysis*

449 Signal peptides were predicted for predicted PHA depolymerases using Signal P 5.0
450 (https://services.healthtech.dtu.dk/service.php?SignalP) with default settings using both Gram-
451 negative and Gram-positive predictions (58). The alignment of amino acid sequences was
452 performed with Clustal Omega from Geneious Prime®2026.0.2 using default settings. Protein
453 conformation was predicted using ColabFold 2 (59). Molecular docking studies were conducted
454 using Autodock 4 (60) to investigate the interaction between the enzyme and its potential
455 substrates. The docking protocol was guided by the crystal structure of the reference protein (PDB
456 ID: 4LIP). Visual representations of the predicted protein structures and docking interactions were
457 generated using PyMOL version 3.0.3 (61).

458 *Construction of B. vietnamiensis LMG 16232 insertional mutants*

459 Genes were interrupted using the RhaCAST method reported previously (31). Briefly, 24
460 bp crRNAs were designed from the genes to be targeted, and the templates were ordered as single-
461 stranded oligos and PCR-amplified using PCR primers 3392 and 3421 to create double-stranded

462 DNA fragments. The PCR products were then introduced into pRhaCAST using Golden Gate
463 cloning with SapI (NEB). The newly constructed plasmids were then transformed into *E. coli*
464 Stbl2. pRhaCAST was then introduced to *B. vietnamiensis* LMG 16232 by tetra-parental mating
465 (31). *E. coli* MM290/pRK2013 helper strain, *E. coli* Stbl2/pRhaCAST with corresponding crRNA,
466 and *E. coli* PIR1/pDonorTp was conjugated into *B. vietnamiensis* LMG 16232 on LB agar plate
467 containing 0.05% rhamnose. The plate was incubated at 37°C for 24 hours. Successful
468 exconjugants were selected on LB plates containing trimethoprim and gentamycin to select against
469 the *E. coli*. Colonies that appeared within 48 h at 37°C were screened by colony PCR. All
470 insertional mutants constructed with RhaCAST were verified by whole genome sequencing using
471 Oxford Nanopore Technologies platforms with v14 library prep chemistry and R10.4.1 flow cells
472 by Plasmidsaurus (Oregon, USA). The genomic sequence of the insertional mutants is available
473 after under BioProject: PRJNA1205771.

474 **Author Contributions**

475 STC and ZLY formulated the ideas and design of the project; and EQ performed GGL
476 performed docking experiment; ZLY, SY and MS designed and created plasmids and mutants;
477 ZLY, SY, MS, RD, and WB performed phenotypic assays; ZLY and AMH performed library prep
478 for Tn-seq. EQ performed gene expression analysis. ZLY and AM processed and analyzed the Tn-
479 seq data; ZLY and STC wrote the manuscript and edited together with SY, EQ, GGL, MS, RD,
480 AMH, AM, WB, RS, DBL, and DFDP; STC, DFDP, DBL, RS, and WB provided financial support
481 and supervised the work.

482 **Acknowledgements and Funding Sources**

483 This work was supported by a Natural Sciences and Engineering Research Council
484 (NSERC) of Canada Discovery Grant to SC and a University of Manitoba Collaborative Research

Program (UCRP) grant to SC and DBL. ZLY was supported by a Research Manitoba and University of Manitoba Graduate Fellowship (UMGF); MS and SY were supported by NSERC Undergraduate Student Research Awards (USRA); AMH was supported by a Cystic Fibrosis Canada studentship and a Canadian Institutes of Health Research (CIHR) Vanier award.

Conflict of Interest Statement

The authors declare no competing financial interests.

References

1. Muneer F, Rasul I, Azeem F, Siddique MH, Zubair M, Nadeem H. 2020. Microbial Polyhydroxyalkanoates (PHAs): Efficient Replacement of Synthetic Polymers. J Polym Environ 28:2301–2323.

2. Li Z, Yang J, Loh XJ. 2016. Polyhydroxyalkanoates: opening doors for a sustainable future. NPG Asia Mater 8:e265–e265.

3. Jendrossek D, Handrick R. 2002. Microbial degradation of polyhydroxyalkanoates. Annu Rev Microbiol 56:403–432.

4. Jendrossek D. 2009. Polyhydroxyalkanoate Granules Are Complex Subcellular Organelles (Carbonosomes). J Bacteriol 191:3195–3202.

5. Knoll M, Hamm TM, Wagner F, Martinez V, Pleiss J. 2009. The PHA Depolymerase Engineering Database: A systematic analysis tool for the diverse family of polyhydroxyalkanoate (PHA) depolymerases. BMC Bioinformatics 10:89.

6. Viljakainen VR, Hug LA. 2021. The phylogenetic and global distribution of bacterial polyhydroxyalkanoate bioplastic-degrading genes. Environ Microbiol 23:1717–1731.

7. Schirmer A, Jendrossek D. 1994. Molecular Characterization of the Extracellular Poly(3-Hydroxyoctanoic Acid) [P(3HO)] Depolymerase Gene of *Pseudomonas fluorescens* GK13 and of Its Gene Product. J Bacteriol 176:7065–7073.

8. Kim DY, Kim HC, Kim SY, Rhee YH. 2005. Molecular characterization of extracellular medium-chain-length poly(3-hydroxyalkanoate) depolymerase genes from *Pseudomonas alcaligenes* strains. J Microbiol Seoul Korea 43:285–294.

9. Rhee YH, Kim YH, Shin K-S. 2006. Characterization of an extracellular poly (3-hydroxyoctanoate) depolymerase from the marine isolate, *Pseudomonas luteola* M13-4. Enzyme Microb Technol 38:529–535.

515 10. Martínez V, de la Peña F, García-Hidalgo J, de la Mata I, García JL, Prieto MA. 2012.
516 Identification and Biochemical Evidence of a Medium-Chain-Length
517 Polyhydroxyalkanoate Depolymerase in the *Bdellovibrio bacteriovorus* Predatory
518 Hydrolytic Arsenal. Appl Environ Microbiol 78:6017–6026.

519 11. Papaneophytou CP, Velali EE, Pantazaki AA. 2011. Purification and characterization of an
520 extracellular medium-chain length polyhydroxyalkanoate depolymerase from *Thermus*
521 *thermophilus* HB8. Polym Degrad Stab 96:670–678.

522 12. Martínez V, de Santos PG, García-Hidalgo J, Hormigo D, Prieto MA, Arroyo M, de la
523 Mata I. 2015. Novel extracellular medium-chain-length polyhydroxyalkanoate
524 depolymerase from *Streptomyces exfoliatus* K10 DSMZ 41693: a promising biocatalyst for
525 the efficient degradation of natural and functionalized mcl-PHAs. Appl Microbiol
526 Biotechnol 99:9605–9615.

527 13. Gangoiti J, Santos M, Prieto MA, de la Mata I, Serra JL, Llama MJ. 2012. Characterization
528 of a Novel Subgroup of Extracellular Medium-Chain-Length Polyhydroxyalkanoate
529 Depolymerases from Actinobacteria. Appl Environ Microbiol 78:7229–7237.

530 14. Santos M, Gangoiti J, Keul H, Möller M, Serra JL, Llama MJ. 2013. Polyester hydrolytic
531 and synthetic activity catalyzed by the medium-chain-length poly(3-hydroxyalkanoate)
532 depolymerase from *Streptomyces venezuelae* SO1. Appl Microbiol Biotechnol 97:211–222.

533 15. Gupta R, Gupta N, Rathi P. 2004. Bacterial lipases: an overview of production, purification
534 and biochemical properties. Appl Microbiol Biotechnol 64:763–781.

535 16. Jaeger KE, Steinbüchel A, Jendrossek D. 1995. Substrate specificities of bacterial
536 polyhydroxyalkanoate depolymerases and lipases: bacterial lipases hydrolyze poly(omega-
537 hydroxyalkanoates). Appl Environ Microbiol 61:3113–3118.

538 17. Sharma PK, Mohanan N, Sidhu R, Levin DB. 2019. Colonization and degradation of
539 polyhydroxyalkanoates by lipase-producing bacteria. Can J Microbiol 65:461–475.

540 18. Rathi P, Saxena RK, Gupta R. 2001. A novel alkaline lipase from *Burkholderia cepacia* for
541 detergent formulation. Process Biochem 37:187–192.

542 19. Oliveira BH, Santos RÉ, Loiola LEA, Nascimento VMG. 2015. Overproduction and
543 properties of lipase by a wild strain of *Burkholderia lata* LBBIO-BL02 using chicken fat. 2.
544 Ann Microbiol 65:865–877.

545 20. Shu Z, Wu J, Chen D, Cheng L, Zheng Y, Chen J, Huang J. 2012. Optimization of
546 *Burkholderia* sp. ZYB002 lipase production for pitch control in thermomechanical pulping
547 (TMP) processes. Holzforschung 66:341–348.

548 21. Lo C-F, Yu C-Y, Kuan I-C, Lee S-L. 2012. Optimization of Lipase Production by
549 *Burkholderia* sp. Using Response Surface Methodology. Int J Mol Sci 13:14889.

550 22. Lang DA, Mannesse ML, de Haas GH, Verheij HM, Dijkstra BW. 1998. Structural basis of
551 the chiral selectivity of *Pseudomonas cepacia* lipase. Eur J Biochem 254:333–340.

552 23. Trodler P, Schmid RD, Pleiss J. 2009. Modeling of solvent-dependent conformational
553 transitions in *Burkholderia cepacia* lipase. BMC Struct Biol 9:38.

554 24. Schrag JD, Li Y, Cygler M, Lang D, Burgdorf T, Hecht HJ, Schmid R, Schomburg D,
555 Rydel TJ, Oliver JD, Strickland LC, Dunaway CM, Larson SB, Day J, McPherson A. 1997.
556 The open conformation of a *Pseudomonas* lipase. Struct Lond Engl 1993 5:187–202.

557 25. Barbe S, Lafaquière V, Guieysse D, Monsan P, Remaud-Siméon M, André I. 2009. Insights
558 into lid movements of *Burkholderia cepacia* lipase inferred from molecular dynamics
559 simulations. Proteins 77:509–523.

560 26. Lee J, Suh SW, Shin S. 2000. Computational studies of essential dynamics of *Pseudomonas*
561 *cepacia* lipase. J Biomol Struct Dyn 18:297–309.

562 27. Yudistira H, McClarty L, Bloodworth RA, Hammond SA, Butcher H, Mark BL, Cardona
563 ST. 2011. Phenylalanine induces *Burkholderia cenocepacia* phenylacetic acid catabolism
564 through degradation to phenylacetyl-CoA in synthetic cystic fibrosis sputum medium.
565 Microb Pathog 51:183–196.

566 28. Tung TT, Quoc Thang N, Cao Huy N, Bao Phuong P, Ngoc Minh D, Hai Nam N, Nielsen
567 J. 2024. Identification of novel phenylalanine derivatives bearing a hydroxamic acid moiety
568 as potent quorum sensing inhibitors. RSC Med Chem 15:1320–1328.

569 29. Yap ZL, Motnenko A, Cardona S. 2023. Complete Genome Sequence of *Burkholderia*
570 *vietnamiensis* LMG16232. Microbiol Resour Announc 12:e0032823.

571 30. Baym M, Shaket L, Anzai IA, Adesina O, Barstow B. 2016. Rapid construction of a whole-
572 genome transposon insertion collection for *Shewanella oneidensis* by Knockout Sudoku.
573 Nat Commun 7:1–13.

574 31. Yap ZL, Rahman ASMZ, Hogan AM, Levin DB, Cardona ST. 2024. A CRISPR-Cas-
575 associated transposon system for genome editing in *Burkholderia cepacia* complex species.
576 Appl Environ Microbiol 90:e00699-24.

577 32. Zeng T, Yin J, Liu Z, Li Z, Zhang Y, Lv Y, Lu M-L, Luo M, Chen M, Xiao Y. 2023.
578 Mechanistic insights into transposon cleavage and integration by TnsB of ShCAST system.
579 Cell Rep 42:112698.

580 33. Erlanson C, Borgström B. 1970. Tributyrine as a substrate for determination of lipase
581 activity of pancreatic juice and small intestinal content. Scand J Gastroenterol 5:293–295.

582 34. Mohanan N, Wong CH, Budisa N, Levin DB. 2022. Characterization of Polymer Degrading
583 Lipases, LIP1 and LIP2 From *Pseudomonas chlororaphis* PA23. Front Bioeng Biotechnol
584 10:854298.

585 35. Knapp A, Voget S, Gao R, Zaburannyi N, Krysciak D, Breuer M, Hauer B, Streit WR,
586 Müller R, Daniel R, Jaeger K-E. 2015. Mutations improving production and secretion of
587 extracellular lipase by *Burkholderia glumae* PG1. Appl Microbiol Biotechnol 100:1265.

588 36. Khattabi ME, Gelder PV, Bitter W, Tommassen J. 2000. Role of the Lipase-specific
589 Foldase of *Burkholderia glumae* as a Steric Chaperone. J Biol Chem 275:26885–26891.

590 37. Sánchez DA, Tonetto GM, Ferreira ML. 2018. *Burkholderia cepacia* lipase: A versatile
591 catalyst in synthesis reactions. Biotechnol Bioeng 115:6–24.

592 38. Liu C-H, Huang C-C, Wang Y-W, Chang J-S. 2012. Optimizing lipase production from
593 isolated *Burkholderia* sp. J Taiwan Inst Chem Eng 43:511–516.

594 39. Li J, Shen W, Fan G, Li X. 2018. Screening, purification and characterization of lipase
595 from *Burkholderia pyrrocinia* B1213. 3 Biotech 8:387.

596 40. Alnoch RC, Cardoso RLA, Guizelini D, Balsanelli E, Tadra-Sfeir MZ, de Oliveira Pedrosa
597 F, Sassaki GL, Cruz LM, Mitchell DA, de Souza EM, Krieger N, Muller-Santos M. 2019.
598 Genome sequencing of *Burkholderia contaminans* LTEB11 reveals a lipolytic arsenal of
599 biotechnological interest. Braz J Microbiol 50:619–624.

600 41. Park O-J, Lee S-H. 2005. Stereoselective lipases from *Burkholderia* sp., cloning and their
601 application to preparation of methyl (*R*)-*N*-(2,6-dimethylphenyl)alaninate, a key
602 intermediate for (*R*)-Metalaxyl. J Biotechnol 120:174–182.

603 42. Lee S-H, Kim M-N. 2010. Isolation of bacteria degrading poly(butylene succinate-*co*-
604 butylene adipate) and their *lip A* gene. Int Biodeterior Biodegrad 64:184–190.

605 43. Nor Azura Azam et al. 2018. Enhanced degradation of polyhydroxyalkanoates (PHAs) by
606 newly isolated *Burkholderia cepacia* DP1 with high depolymerase activity. 27 Apri 2017
607 75:11.

608 44. Azura Azami N, Ira Aryani W, Aik-Hong T, Amirul AA. 2019. Purification and
609 characterization of new bio-plastic degrading enzyme from *Burkholderia cepacia* DP1.
610 Protein Expr Purif 155:35–42.

611 45. Cuthbertson L, Nodwell JR. 2013. The TetR Family of Regulators. Microbiol Mol Biol Rev
612 77:440–475.

613 46. Kniewel R, Revelles Lopez O, Prieto MA. 2017. Biogenesis of Medium-Chain-Length
614 Polyhydroxyalkanoates, p. 1–25. *In* Geiger, O (ed.), Biogenesis of Fatty Acids, Lipids and
615 Membranes. Springer International Publishing, Cham.

616 47. Black PN, DiRusso CC. 1994. Molecular and biochemical analyses of fatty acid transport,
617 metabolism, and gene regulation in *Escherichia coli*. Biochim Biophys Acta 1210:123–145.

618 48. Jimenez-Diaz L, Caballero A, Segura A. 2017. Pathways for the Degradation of Fatty Acids
619 in Bacteria, p. 1–23. *In* Rojo, F (ed.), Aerobic Utilization of Hydrocarbons, Oils and Lipids.
620 Springer International Publishing, Cham.

621 49. Gislason AS, Turner K, Domaratzki M, Cardona ST. 2017. Comparative analysis of the
622 *Burkholderia cenocepacia* K56-2 essential genome reveals cell envelope functions that are
623 uniquely required for survival in species of the genus *Burkholderia*. Microb Genomics
624 3:e000140.

625 50. Cardona ST, Mueller C, Valvano MA. 2006. Identification of essential operons in
626 *Burkholderia cenocepacia* with a rhamnose inducible promoter. Appl Environ Microbiol
627 72:2547–2555.

628 51. Gallagher LA, Shendure J, Manoil C. 2011. Genome-scale identification of resistance
629 functions in *Pseudomonas aeruginosa* using Tn-seq. mBio 2:e00315-10.

630 52. Martin M. 2011. Cutadapt removes adapter sequences from high-throughput sequencing
631 reads. 1. EMBnet.journal 17:10–12.

632 53. Li H, Durbin R. 2010. Fast and accurate long-read alignment with Burrows–Wheeler
633 transform. Bioinformatics 26:589–595.

634 54. Li H, Handsaker B, Wysoker A, Fennell T, Ruan J, Homer N, Marth G, Abecasis G, Durbin
635 R, Subgroup 1000 Genome Project Data Processing. 2009. The Sequence Alignment/Map
636 format and SAMtools. Bioinformatics 25:2078–2079.

637 55. Fu J, Sharma U, Sparling R, Cicek N, Levin DB. 2014. Evaluation of medium-chain-length
638 polyhydroxyalkanoate production by *Pseudomonas putida* LS46 using biodiesel by-product
639 streams. Can J Microbiol 60:461–468.

640 56. Braunegg G, Sonnleitner B, Lafferty RM. 1978. A rapid gas chromatographic method for
641 the determination of polyhydroxybutyric acid in microbial biomass. Eur J Appl Microbiol
642 Biotechnol 6:29–37.

643 57. Blunt W, Lagassé A, Harvey J, Sparling R, Gapes D, Levin D, Cicek N. 2024. Semi-
644 continuous non-sterile production of medium chain-length polyhydroxyalkanoates from
645 fatty acids. Can J Chem Eng 102:3896–3908.

646 58. Almagro Armenteros JJ, Tsirigos KD, Sønderby CK, Petersen TN, Winther O, Brunak S,
647 von Heijne G, Nielsen H. 2019. SignalP 5.0 improves signal peptide predictions using deep
648 neural networks. Nat Biotechnol 37:420–423.

649 59. Kim G, Lee S, Levy Karin E, Kim H, Moriwaki Y, Ovchinnikov S, Steinegger M, Mirdita
650 M. 2025. Easy and accurate protein structure prediction using ColabFold. Nat Protoc
651 20:620–642.

652 60. Morris GM, Huey R, Lindstrom W, Sanner MF, Belew RK, Goodsell DS, Olson AJ. 2009.
653 AutoDock4 and AutoDockTools4: Automated docking with selective receptor flexibility. J
654 Comput Chem 30:2785–2791.

655 61. DeLano WL. 2002. Pymol: An open-source molecular graphics tool. CCP4 Newsl Protein
656 Crystallogr.

657 62. Darling P, Chan M, Cox AD, Sokol PA. 1998. Siderophore production by cystic fibrosis
658 isolates of *Burkholderia cepacia*. Infect Immun 66:874–877.

659 63. Bloodworth RA, Gislason AS, Cardona ST. 2013. *Burkholderia cenocepacia* conditional
660 growth mutant library created by random promoter replacement of essential genes.
661 MicrobiologyOpen 2:243–258.

662 64. Figurski DH, Helinski DR. 1979. Replication of an origin-containing derivative of plasmid
663 RK2 dependent on a plasmid function provided in trans. Proc Natl Acad Sci U S A
664 76:1648–1652.

665

666

667 **Figures and Legends**

668

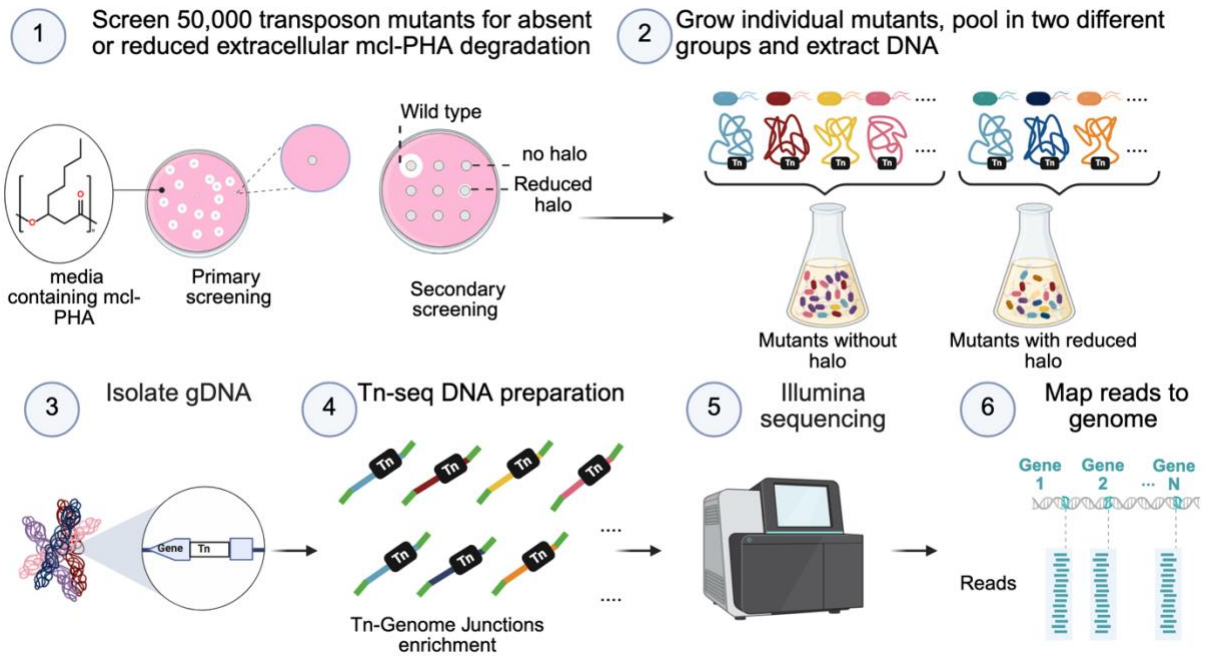

669

670 **Fig 1.** Overview of transposon mutagenesis and Tn-seq workflow to identify genetic elements
671 involved in the extracellular mcl-PHA degradation activity in *B. vietnamiensis* LMG 16232. *B.*
672 *vietnamiensis* LMG 16232 was subjected to transposon mutagenesis, and 50,000 colonies were
673 screened for those with absent or reduced extracellular mcl-PHA degradation activity. Colonies
674 showing reduced or no degradation activity were selected for further analysis. Selected mutants
675 were grown individually and then grouped into two pools based on their mcl-PHA degradation
676 activity (Pool 1 for no activity, Pool 2 for weak activity). Genomic DNA (gDNA) was extracted
677 from each pool. The gDNA was prepared for Tn-Genome junction enrichment. The enriched DNA
678 fragments were sequenced using Illumina MiSeq. The sequencing data were analyzed by mapping
679 the reads to the *B. vietnamiensis* LMG 16232 genome.

680

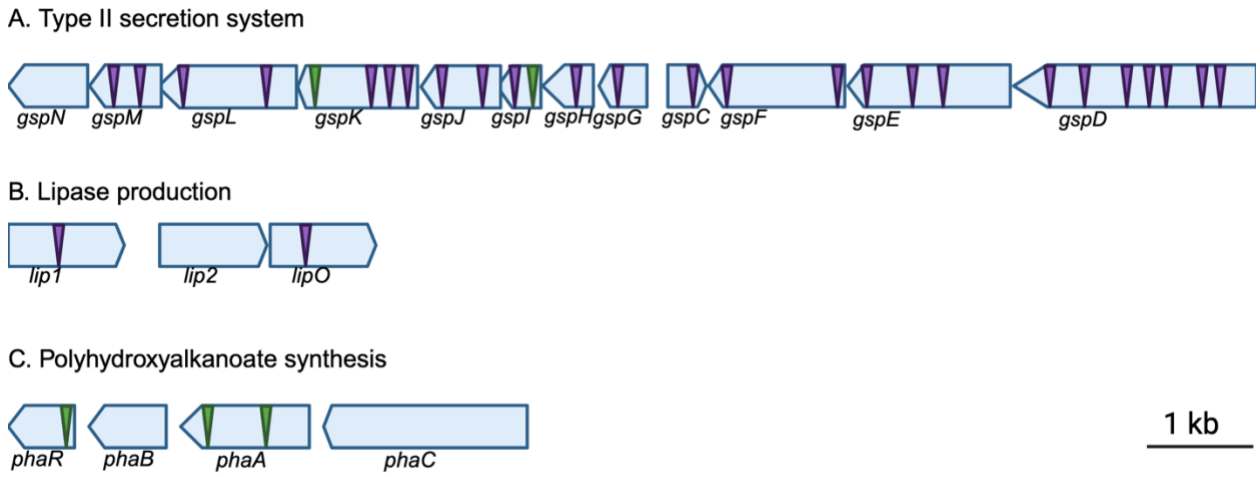

Fig 2. Genetic Organization of the *B. vietnamiensis* LMG 16232 gene clusters that affect the extracellular mcl-PHA when disrupted by transposon insertions . Triangles indicate transposon insertions that resulted in complete loss (purple) or severe reduction (green) of extracellular mcl-PHA degradation activity in *B. vietnamiensis* LMG 16232; **A**) The T2SS of *B. vietnamiensis* LMG 16232 arranges in a gene cluster containing 12 genes (P4G95_05480, P4G95_05485, P4G95_05490, P4G95_05495, P4G95_05500, P4G95_05505, P4G95_05510, P4G95_05515, P4G95_05520, P4G95_05525, P4G95_05530, P4G95_05535). All genes of the gene cluster are interrupted except for *gspN*; **B**) lipase gene cluster consists of three genes, *lip1, lip2* and *lipO* (P4G95_16805, P4G95_16810, and P4G95_16815); **C**) The polyhydroxyalkanoate synthesis gene cluster of *B. vietnamiensis* LMG 16232 consists of four genes, *phaR, phaB, phaA, and phbC* (P4G95_13560, P4G95_13565, P4G95_13570, and P4G95_13575). The genes are depicted to scale, as indicated by the bars on the right side of the panels. The putative function of transposon-disrupted genes is provided in Table 2.

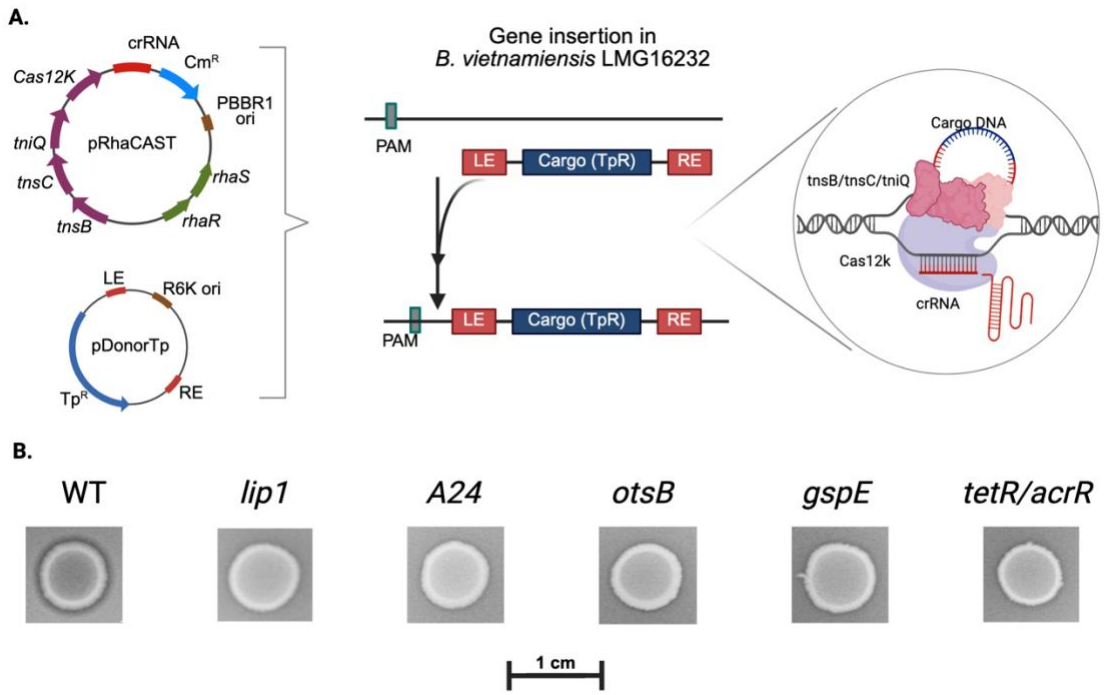

Fig 3. Targeting genes involved in mcl-PHA degradation in *B. vietnamiensis* LMG 16232 abolish the strain's ability to degrade mcl-PHA; **A**) Schematic model of RNA-guided DNA transposition by RhaCAST applied to *B. vietnamiensis* LMG 16232. The two plasmids of the RhaCAST system, pRhaCAST and pDonorTp, encode all the necessary components, *tnsB*, *tnsC*, *tniQ*, Cas12k, crRNA scaffold, and the cargo gene (TpR) that is flanked by the transposon left end (LE) and right end (RE); **B**) Bacterial growth on PHO plates of WT and RhaCAST mutants. Images are croppings from a representative PHO agar plate. The scale bar (1 cm) is shown for size reference. WT, B. vietnamiensis LMG 16323. *Lip 1,* A24, *otsB, gspE* and *tetR/acrR* are the targeted genes. Putative functions are described in Table 2. Complete name of the mutants is provided in Table 3.

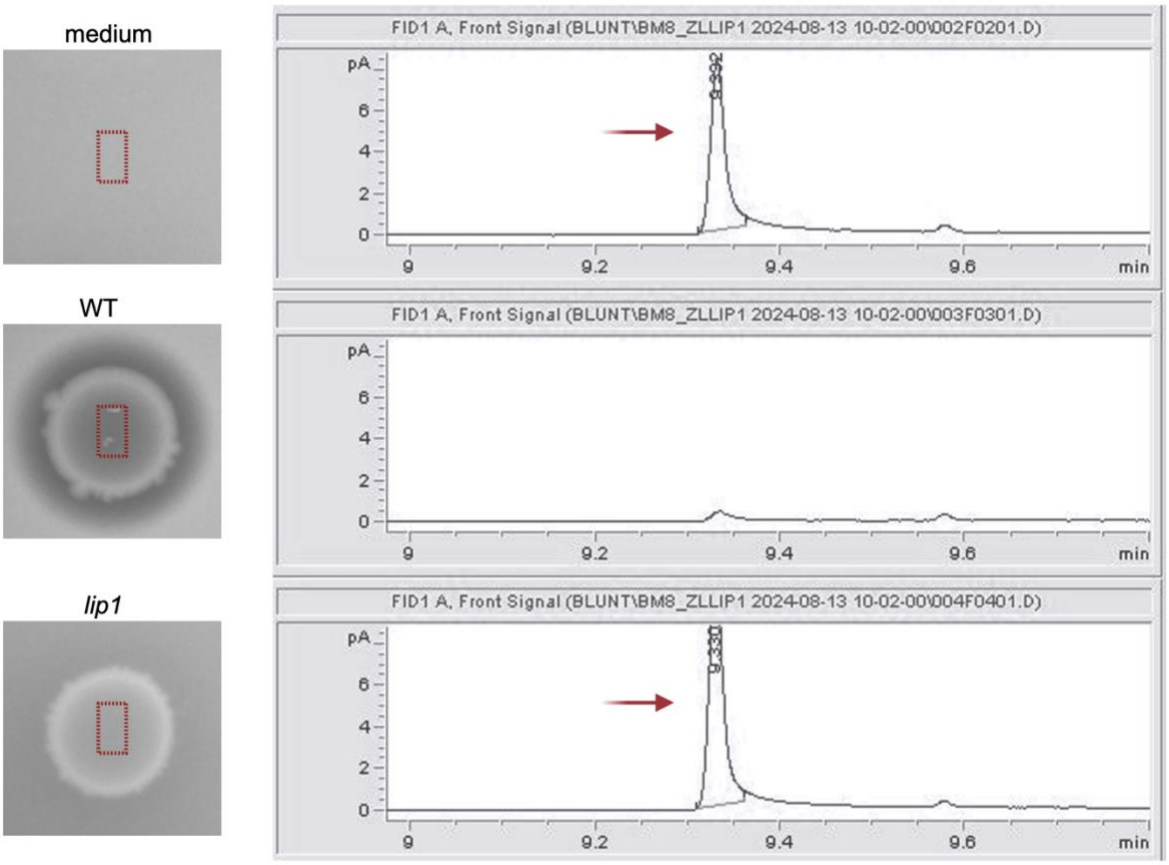

705

706 **Fig 4.** Targeting the putative *lipase* gene (locus tag: P4G95_16805) in *B. vietnamiensis* LMG
707 16232 abolishes the ability to degrade mcl-PHA. The absence or presence of PHO in the agar after
708 strain inoculation was determined with gas chromatography with flame ionization detection (GC-
709 FID). Samples were obtained by cutting an agar disk under the strain. For control, a disk was cut
710 at an area of the agar where no cell was inoculated. The peak at ~9.3 minutes retention time
711 corresponds to PHO, which can be observed at the no cell control (Top). The absence of a peak
712 corresponds to PHO in WT, and the presence of PHO underneath the *lip1* mutant growth supports
713 the phenotypic test. Strains were grown on an agar plate containing Nile red and PHO and
714 visualized under UV irradiation. Inoculation of wild type (WT) results in a clear halo around the
715 strain, whereas the inoculation of the *lip1* mutant does not have a halo around the strain.

716

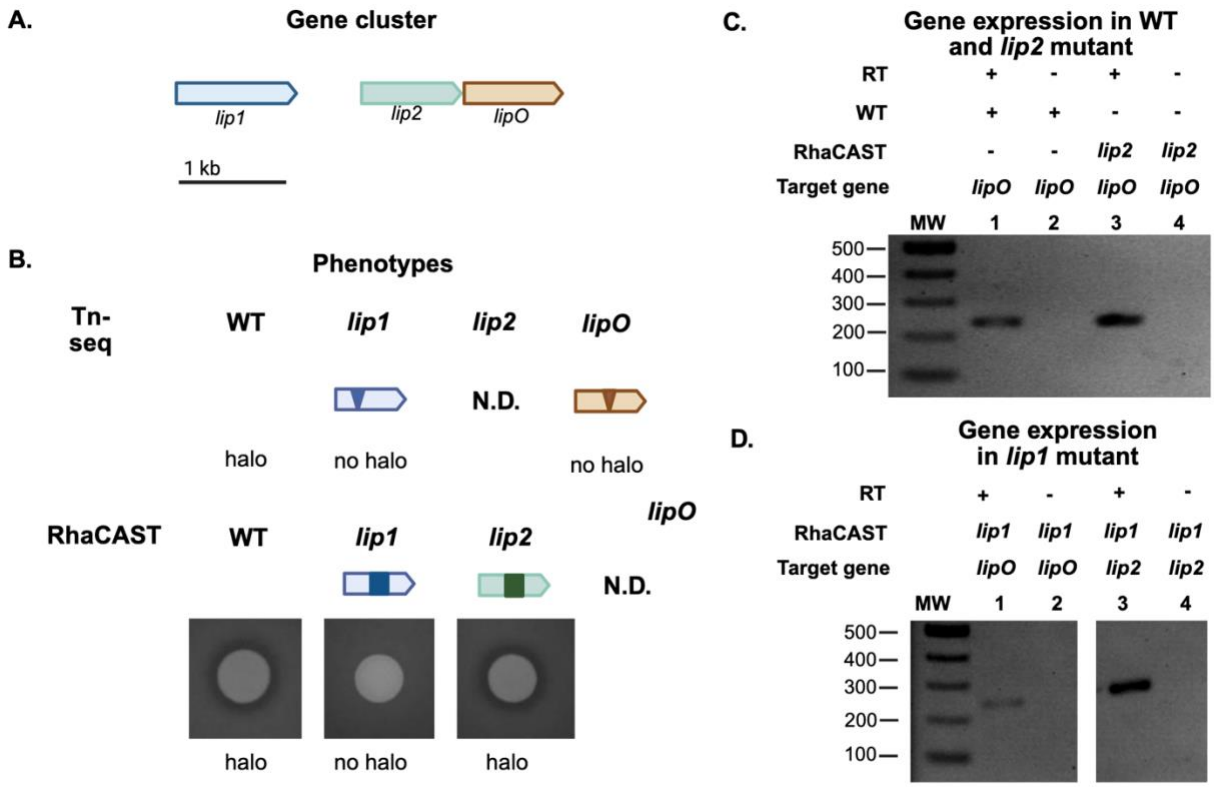

Fig. 5. Phenotypic and gene expression analysis of the lipase production gene cluster. **A**) Scheme of the *B. vietnamiensis* LMG 16232 *lip1, lip2* and *lipO* (P4G95_16805, P4G95_16810, and P4G95_16815); **B**) mcl-PHA degradation phenotypes of the respective mutants produced by Tn-seq (scheme) or RhaCAST (bacterial growth on PHO plates after 7 days); **C-D)** Lipase cluster expression analysis. WT, *lip1* and *lip2* mutants were grown on PHO plates and at day 0 (shown) 4 and 7, cells were harvested for RNA extraction. Expression of target genes was confirmed by RT-PCR. RT, reverse transcriptase.

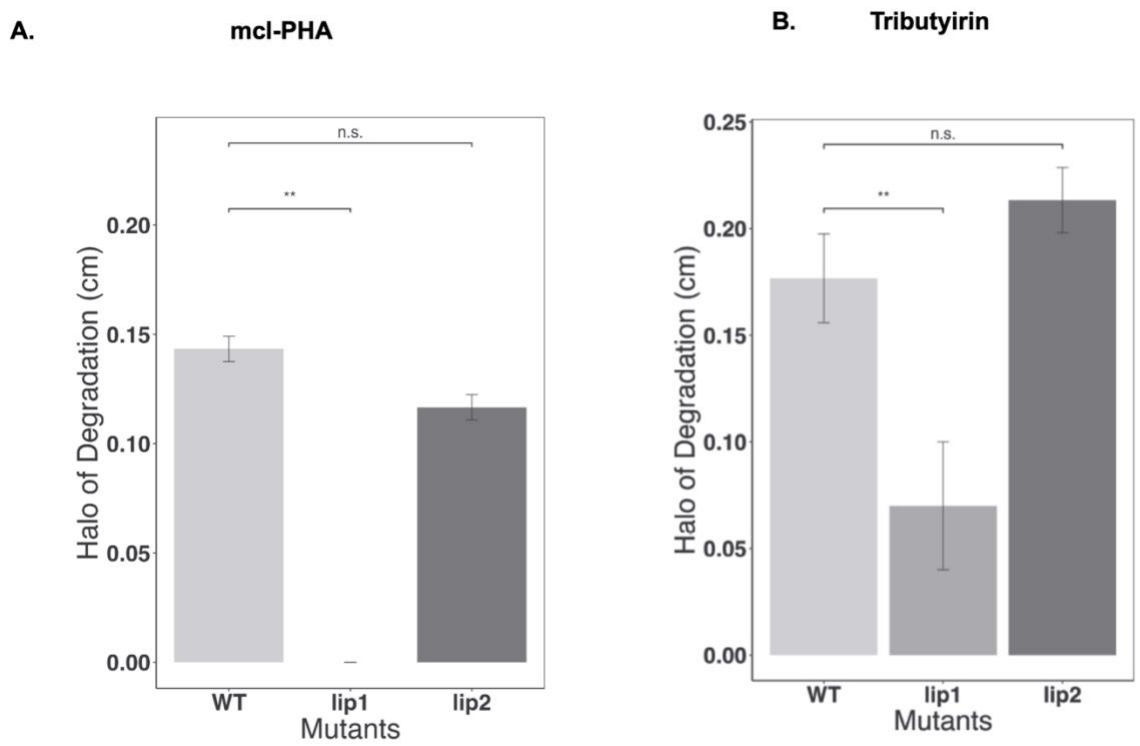

Fig 6. Quantification of mcl-PHA and tributyrin degradation in *B. vietnamiensis* LMG 16232, *lip1* and *lip2* mutants. Diameter of the halos degradation in **A**) mcl-PHA or **B**) tributyrin. Strains were grown on an agar plate supplemented with tributyrin for 3 days or mcl-PHA for 7 days at 37ºC. Data is representative of three biological replicates repeated in technical duplicates.

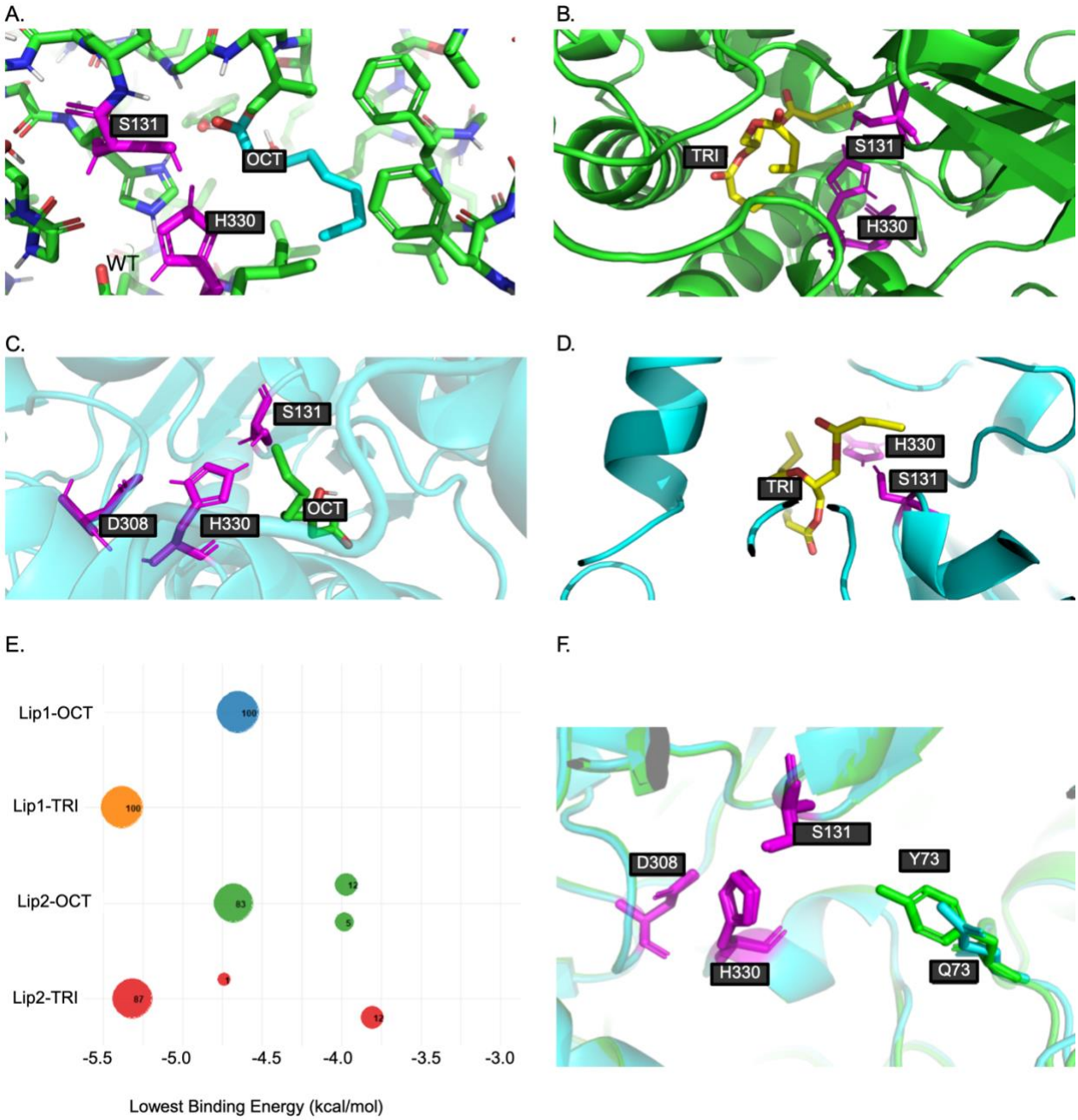

734

735 **Fig. 7.** Docking analysis of Lip1 and Lip2-substrate complexes. **A**) Docking poses of Lip1 with 3-
736 Hydroxyoctanoate (OCT); **B**) Docking poses of Lip1 with Tributyrin (TRI); **C**) Docking poses of
737 Lip2 with 3-Hydroxyoctanoate (OCT); **D**) Docking poses of Lip2 with Tributyrin (TRI). The
738 images illustrate the single predominant low-energy binding cluster obtained for both substrates,

739 highlighting the catalytic triad in violet; **E**) Binding energy and cluster distribution for protein-
740 ligand complexes. The plot shows the lowest binding energy for Lip1 and Lip2 docking with 3-
741 Hydroxyoctanoate (OCT) and Tributyrin (TRI). The size of the circle represents the cluster size
742 (number of poses), while colours differentiate protein-ligand pairs: Lip1-OCT (blue), Lip1-TRI
743 (orange), Lip2-OCT (green), and Lip2-TRI (red). Lip1 exhibits a higher affinity for both ligands,
744 characterized by a single predominant low-energy cluster, whereas Lip2 displays multiple binding
745 modes for both substrates; **F**) Structural superposition of Lip1 and Lip2 at amino acid at position
746 73. Superposition of Lip1 (green) and Lip2 (blue), highlighting the catalytic triad (violet) and the
747 difference in amino acid in position 73: Lip1 (tyrosine, Y) and Lip2 (glutamine, Q), illustrating its
748 potential impact on enzyme structure and function.

749

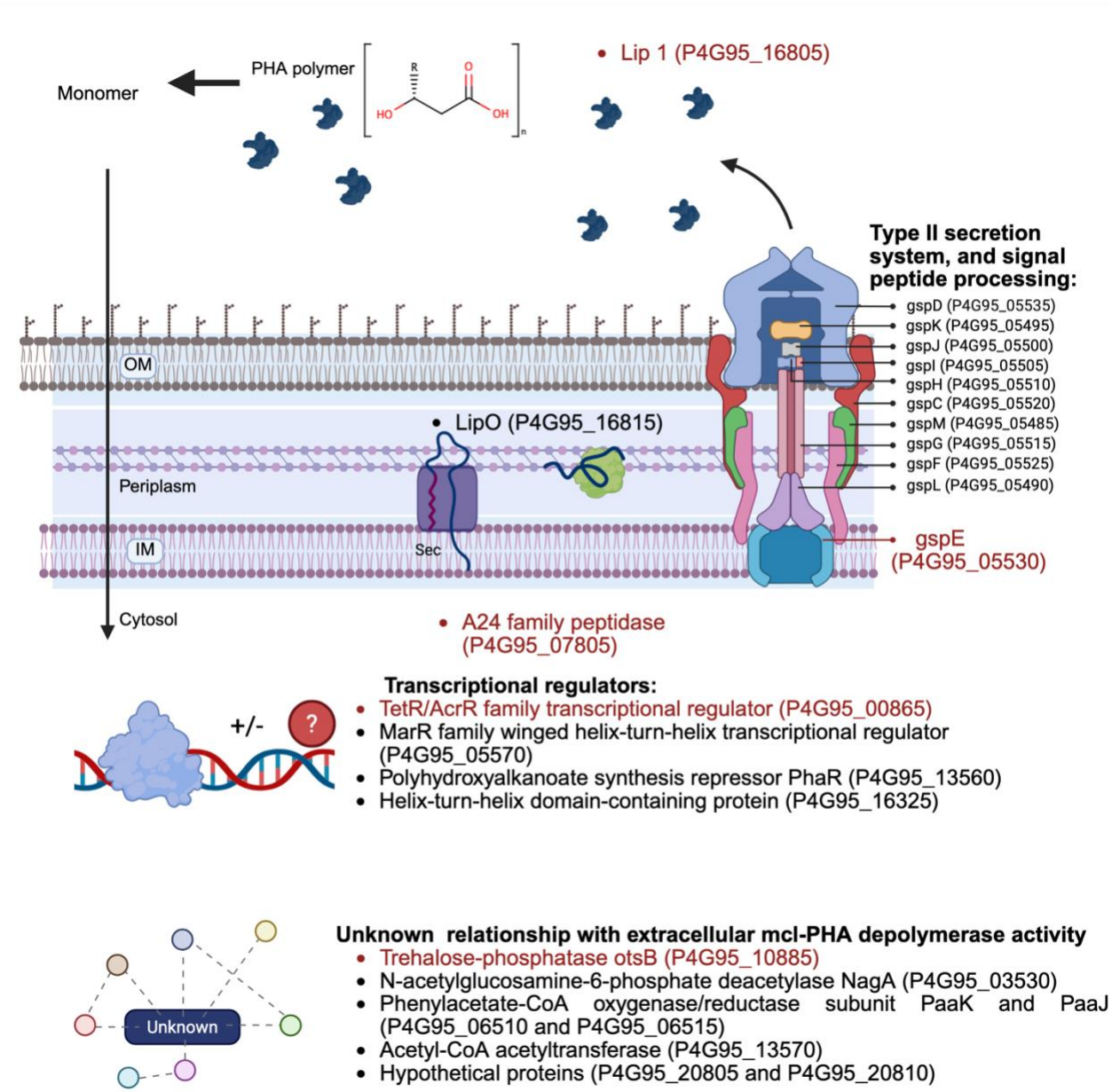

Fig 8. Proposed model of components involved in *B. vietnamiensis* LMG 16232 extracellular mcl-PHA degradation activity. The elements in this model were deduced from the transconjugants that either lost or showed severely reduced extracellular mcl-PHA depolymerase activity due to transposon insertion. The components where the text is in red have been verified via the creation of insertional mutagenesis using RhaCAST. The regulatory elements influencing this activity are TetR/AcrR family transcriptional regulator (P4G95_00865), Polyhydroxyalkanoate synthesis

757 repressor (P4G95_13560) and HTH-type regulators (P4G95_05570 and P4G95_16325). The Sec
758 system is responsible for transporting the unfolded protein into the periplasmic, as the protein is
759 predicted to contain a sec tag. The putative lipase chaperone (P4G95_16815) is responsible for
760 folding the putative lipase into a mature protein and excreted to the outside of the cell via the T2SS.
761 *B. vietnamiensis* LMG 16232 extracellular mcl-PHA degradation activity is also affected by the
762 transposon interruption in genetic elements related to polyhydroxyalkanoate production and
763 several genes involved in metabolism.
764

765

Table 1. *Burkholderia* isolates that exhibit extracellular mcl-PHO degradation activity

Species	Strain	Ability to degrade PHO	
		30 ˚C	37 ˚C
Burkholderia cenocepacia	K56-2	-	-
	F9141525	-	-
	F3071909	-	-
	G1181568-1	-	-
	F4200989-3	-	-
	VC14488	-	-
	VC14543	-	-
	VC10414	-	-
	VC14761	-	-
	130723	-	-
	125007	-	-
Burkholderia contaminans	21NG595759	-	-
	21NG609698	-	-
Burkholderia dolosa	AU6940	-	-
	AU2167	-	-
	LM018941	-	-
	AU0645	-	-
Burkholderia gladioli	VC19233	+	+
	VC14812	-	-
	132208	+	-
	113611	-	-
Burkholderia multivorans	21NH942533	+	+
	21NJ503211	+	-
	V1120157	-	-
	LM013010	-	-
	F9091687	+	-
	VC19694	-	-
	VC15555	-	-
	VC9825	+	+
	131077	-	-
Burkholderia stagnalis	MSMB618	++	++
	MSMB642	++	++
Burkholderia vietnamiensis	LMG 22486	-	-
	LMG 10929	-	-
	LMG 16232	++	++
	VC11431	-	-
	VC18984	-	-

766 mcl-PHA degradation after 20 days was ranked based on (–) no clearing, (+) weak clearing: faint
767 or barely visible halo around the colony, (++) moderate clearing: clearly visible halo with more
768 defined edges. **Fig. S1** is the source of the data interpretation.

Table 2. Transposon mutants of *B. vietnamiensis* LMG 16232 with abolished (Pool 1) or reduced (Pool 2) extracellular mcl-PHA activity

Chromosome number	Locus tag	Number of unique insertions per gene	Gene name/protein name	Putative function
Pool 1				
1	P4G95_00865	3	*tetR*/AcrR family transcriptional regulator	TetR/AcrR family transcriptional regulator
1	P4G95_05485	2	*gspM*	T2SS protein M
1	P4G95_05490	2	*gspL*	T2SS protein GspL
1	P4G95_05495	3	*gspK*	T2SS minor pseudopilin GspK
1	P4G95_05500	2	*gspJ*/prepilin-type N-terminal cleavage/methylation domain-containing protein	prepilin-type N-terminal cleavage/methylation domain-containing protein
1	P4G95_05505	1	*gspI*	T2SS minor pseudopilin GspI
1	P4G95_05510	1	*gspH*/*fimT* family pseudopilin	GspH/FimT family pseudopilin
1	P4G95_05515	1	*gspG*	T2SS major pseudopilin GspG
1	P4G95_05520	1	general secretion pathway protein	general secretion pathway protein GspC CDS
1	P4G95_05525	2	*gspF*	T2SS inner membrane protein GspF
1	P4G95_05530	3	*gspE*	T2SS ATPase GspE
1	P4G95_05535	7	*gspD*	T2SS secretin GspD
1	P4G95_07805	3	A24 family peptidase	A24 family peptidase
1	P4G95_10885	1	*otsB*	trehalose-phosphatase
2	P4G95_16805	1	l*ip1*/triacylglycerol lipase	triacylglycerol lipase
2	P4G95_16815	1	*lipO*/lipase secretion chaperone	lipase secretion chaperone
2	P4G95_20805	1	hypothetical protein	hypothetical protein
3	P4G95_28980	1	*gspD*	T2SS secretion GspD
Pool 2				
1	P4G95_03530	1	*nagA*	N-acetylglucosamine-6-phosphate deacetylase

1	P4G95_05495	1	*gspK*	T2SS minor pseudopilin GspK
1	P4G95_05505	1	*gspI*	T2SS minor pseudopilin GspI
1	Between P4G95_05555 and P4G95_05560	1	Between *mnmC* and cation:proton antiporter CDS	cation:proton antiporter
1	P4G95_05570	1	*MarR* family winged helix-turn-helix transcriptional regulator	MarR family winged helix-turn-helix transcriptional regulator
1	P4G95_06510 and P4G95_06515	1	*paaK* and *paaJ*	phenylacetate-CoA oxygenase/reductase subunit PaaK and phenylacetate-CoA oxygenase subunit PaaJ
1	P4G95_13560	1	*phaR*	polyhydroxyalkanoate synthesis repressor PhaR
1	P4G95_13570	2	acetyl-CoA C-acetyltransferase	acetyl-CoA C-acetyltransferase
1	Between P4G95_15285 and P4G95_15290	1	Between cupin domain-containing protein CDS and hypothetical protein	
2	P4G95_16325	1	helix-turn-helix domain-containing protein	helix-turn-helix domain-containing protein
2	P4G95_20810	1	hypothetical protein	hypothetical protein
3	Between P4G95_29770 and P4G95_29775	2	Between porin CDS and helix-turn-helix domain-containing protein CDS	

769

770

771 **Table 3.** List of bacterial strains and plasmids used in this work.

Strain or plasmid	Features	Source
Burkholderia cenocepacia K56-2	ET12 lineage cystic fibrosis clinical isolate from Toronto	(62)
Burkholderia cenocepacia F9141525	Cystic fibrosis clinical isolate from Toronto	SickKids, Toronto
Burkholderia cenocepacia F3071909	Cystic fibrosis clinical isolate from Toronto	SickKids, Toronto
Burkholderia cenocepacia G1181568-1	Cystic fibrosis clinical isolate from Toronto	SickKids, Toronto
Burkholderia cenocepacia F4200989-3	Cystic fibrosis clinical isolate from Toronto	SickKids, Toronto
Burkholderia cenocepacia VC14488	Canadian cystic fibrosis isolate	CBCCRRR
Burkholderia cenocepacia VC14543	Canadian cystic fibrosis isolate	CBCCRRR
Burkholderia cenocepacia VC10414	Canadian cystic fibrosis isolate	CBCCRRR
Burkholderia cenocepacia VC14761	Canadian cystic fibrosis isolate	CBCCRRR
Burkholderia cenocepacia 130723	Clinical respiratory isolated collected in Halifax	CANWARD/CARA database
Burkholderia cenocepacia 125007	Clinical respiratory isolated collected in Vancouver	CANWARD/CARA database
Burkholderia contaminans 21NG595759	Canadian cystic fibrosis isolate	H. Adam (Shared Health MB)
Burkholderia contaminans 21NG609698	Canadian cystic fibrosis isolate	H. Adam (Shared Health MB)
Burkholderia dolosa AU6940	Cystic fibrosis clinical isolate	SickKids, Toronto
Burkholderia dolosa AU2167	Cystic fibrosis clinical isolate	SickKids, Toronto
Burkholderia dolosa LM018941	Cystic fibrosis clinical isolate	SickKids, Toronto
Burkholderia dolosa AU0645	Cystic fibrosis clinical isolate	SickKids, Toronto
Burkholderia gladioli VC19233	Canadian cystic fibrosis isolate	CBCCRRR
Burkholderia gladioli VC14812	Canadian cystic fibrosis isolate	CBCCRRR
Burkholderia gladioli 132208	Clinical respiratory isolated collected in Montreal	CANWARD/CARA database

Burkholderia gladioli 113611	Clinical respiratory isolated collected in Saskatoon	CANWARD/CARA database
Burkholderia multivorans 21NH942533	Canadian cystic fibrosis isolate	H. Adam (Shared Health MB)
Burkholderia multivorans 21NJ503211	Canadian cystic fibrosis isolate	H. Adam (Shared Health MB)
Burkholderia multivorans V1120157	Cystic fibrosis clinical isolate	SickKids, Toronto
Burkholderia multivorans LM013010	Cystic fibrosis clinical isolate	SickKids, Toronto
Burkholderia multivorans F9091687	Cystic fibrosis clinical isolate	SickKids, Toronto
Burkholderia multivorans VC19694	Canadian cystic fibrosis isolate	CBCCRRR
Burkholderia multivorans VC15555	Canadian cystic fibrosis isolate	CBCCRRR
Burkholderia multivorans VC9825	Canadian cystic fibrosis isolate	CBCCRRR
Burkholderia multivorans 131077	Clinical respiratory isolated collected in Toronto	CANWARD/CARA database
Burkholderia stagnalis MSMB618	N/A	NAU-PMI
Burkholderia stagnalis MSMB642	N/A	NAU-PMI
Burkholderia vietnamiensis LMG 22486	Wastewater isolate	BCCM
Burkholderia vietnamiensis LMG 10929	Oryza sativa, rhizosphere soil isolate	BCCM
Burkholderia vietnamiensis LMG 16232	Clinical isolate from cystic fibrosis patient	BCCM
Burkholderia vietnamiensis VC11431	Canadian cystic fibrosis isolate	CBCCRRR
Burkholderia vietnamiensis VC18984	Canadian cystic fibrosis isolate	CBCCRRR
Burkholderia vietnamiensis LMG 16232 *lip1*::CAST-Tp *(lip1)*	Derived from LMG 16232; Cargo containing Tp^r integrated into triacylglycerol lipase CDS (P4G95_16805), created with crRNA 3668, distance from protospacer adjacent motif (PAM): 63	This study
Burkholderia vietnamiensis LMG 16232 *lip2*::CAST-Tp *(lip2)*	Derived from LMG 16232; Cargo containing Tp^r integrated into triacylglycerol lipase CDS (P4G95_16810), created with crRNA	This study

	3890, distance from protospacer adjacent motif (PAM): 66	
Burkholderia vietnamiensis LMG 16232 A24 family peptidase CDS:: CAST-Tp (*A24*)	Derived from LMG 16232; Cargo containing Tp^r integrated into A24 family peptidase CDS (P4G95_07805), created with crRNA 3952, distance from PAM: 64	This study
Burkholderia vietnamiensis LMG 16232 *otsB*::CAST-Tp (*otsB*)	Derived from LMG 16232; Cargo containing Tp^r integrated into *otsB* (P4G95_10885), created with crRNA 3956 distance from PAM: 65	This study
Burkholderia vietnamiensis LMG 16232 *gspE*::CAST-Tp *gspE*	Derived from LMG 16232; Cargo containing Tp^r integrated into *gspE* (P4G95_05530), created with crRNA 3996, distance from PAM: 63	This study
Burkholderia vietnamiensis LMG 16232 TetR/AcrR family transcriptional regulator CDS::CAST-Tp (*tetR/acrR*)	Derived from LMG 16232; Cargo containing Tp^r integrated into TetR/AcrR family transcriptional regulator CDS (P4G95_00865), created with crRNA 4000, distance from PAM: 126	This study
E. coli Stbl2	*F- mcrA Δ(mcrBC-hsdRMS-mrr) recA1 endA1lon gyrA96 thi supE44 relA1* λ^- *Δ(lac-proAB)*	Invitrogen
pRBrhaBoutgfp	pSCrhaBoutgfp derivative, ori_{R6K}, *rhaR rhaS* PrhaB e-gfp	(63)
pRK2013	ori_{colE1} RK2 derivative Kan^r mob^+ tra^+	(64)
pDonorTp	pDonor_ShCAST_kanR with modification of Km^R to Tp^R	(31)
pRhaCAST	*Sh-cas12K-tnsBC-tniQ* drives by the rhamnose inducible promoter	(31)
pRhaCAST-3668	Modified from pRhaCAST. crRNA targeting *B. vietnamiensis* LMG 16232 triacylglycerol lipase CDS (P4G95_16805)	This study
pRhaCAST-3952	Modified from pRhaCAST. crRNA targeting *B. vietnamiensis* LMG 16232 A24 family peptidase CDS (P4G95_07805)	This study
pRhaCAST-3956	Modified from pRhaCAST. crRNA targeting *B. vietnamiensis* LMG 16232 *otsB* (P4G95_10885)	This study
pRhaCAST-3996	Modified from pRhaCAST. crRNA targeting *B. vietnamiensis* LMG 16232 *gspE* (P4G95_05530)	This study

pRhaCAST-4000	Modified from pRhaCAST. crRNA targeting *B. vietnamiensis* LMG 16232 TetR/AcrR family transcriptional regulator CDS (P4G95_00865)	This study

772

773 **Table 4.** Primers/templates used in this study

Number	Sequence	Description
Oligonucleotides for Tn-seq		
683	CCGTAGTGAGTTCTTCGTCCGAGCCACTCGGAGATGTGTATAAGAGACAGT	Tn-seq adapter (top strand)
684	CTGTCTCTTATACACATCTCCGAGTGGCTCGGACGAAGAACTCACTACGG	Tn-seq adapter (bottom strand)
682	CACAAGTGCGGCCGCACTAGTCTAGATTTAAATTACCGTAGTGAGTTCTTCGTCCGAGCCAC	Tn-seq oligo probe
681	CAAGCAGAAGACGGCATACGAGATTCGCCTTAGTCTCGTGGGCTCGGAGATGTGTATAAGAGACAG	Illumina Nextera index N701 (Pool 1)
690	AATGATACGGCGACCACCGAGATCTACACTAGATCGCTCGTCGGCAGCGTCAGATGTGTATAAGAGACAGNNNNAATCTAGACTAGTGCGGCC	Illumina Nextera index N501 (Pool 1)
718	CAAGCAGAAGACGGCATACGAGATAGGAGTCCGTCTCGTGGGCTCGGAGATGTGTATAAGAGACAG	Illumina Nextera index N705 (Pool 2)
719	AATGATACGGCGACCACCGAGATCTACACCTCTCTATTCGTCGGCAGCGTCAGATGTGTATAAGAGACAGNNNNAATCTAGACTAGTGCGGCC	Illumina Nextera index N502 (Pool 2)
Oligonucleotides for cloning crRNA into pRhaCAST (crRNA is in bold, *sapI* restriction site is in italics)		
3392	ACTAACGGCTCTTCGAG	Reverse primer to amplify single stranded nucleotide template containing the crRNA
3421	CATTGGCTCTTCGAAAG	Forward primer to amplify single stranded nucleotide template containing the crRNA
3668	CATT*GGCTCTTC*GAAAG**ATCCTCGTGCACGGCCTTACCGGC**GGCTC*GAAGAGC*CGTTAGT	Targeting triacylglycerol lipase 1 CDS (P4G95_16805) of LMG 16232
3890	CATT*GGCTCTTC*GAAAG**GCGAATCTGTCGGCGTTCCAGAGC**GGCTC*GAAGAGC*CGTTAGT	Targeting triacylglycerol lipase 2 CDS (P4G95_16810) of LMG 16232
3952	CATT*GGCTCTTC*GAAAG**GTGATCGGTCTGTGCGTCGGCAGC**GGCTC*GAAGAGC*CGTTAGT	Targeting A24 family peptidase CDS (P4G95_07805) of LMG 16232

3956	CATT*GGCTCTTC*GAAAG**CCTGACCG ATACCGCGTTCTTTTT**GGCTC*GAAG AGC*CGTTAGT	Targeting *otsB* (P4G95_10885) of LMG 16232
3996	CATT*GGCTCTTC*GAAAG**TGCAAGGA AGAGCGACACGAGGAC**GGCTC*GAA GAGC*CGTTAGT	Targeting *gspE* (P4G95_05530) of LMG 16232
4000	CATT*GGCTCTTC*GAAAG**CCACCATCG ACGAGACCTGGTCGT**GGCTC*GAAGA GC*CGTTAGT	Targeting TetR/AcrR family transcriptional regulator CDS (P4G95_00865) of LMG 16232
Oligonucleotides for colony PCR to verify genomic insertion		
3001	GGTGGGTTGAAAGCAAGTCC	left end of the cargo insertion
3670	CTATCCGGTCATCCTCGTGC	Colony PCR for triacylglycerol lipase CDS (P4G95_16805) of LMG 16232
3953	GTGATCGGTCTGTGCGTCG	Colony PCR for A24 family peptidase CDS (P4G95_07805) of LMG 16232
3957	CTGACCGATACCGCGTTCTT	Colony PCR for *otsB* (P4G95_10885) of LMG 16232
3997	GCAAGGAAGAGCGACACGAG	Colony PCR for *gspE* (P4G95_05530) of LMG 16232
4001	CCACCATCGACGAGACCTG	Colony PCR for TetR/AcrR family transcriptional regulator CDS (P4G95_00865) of LMG 16232
Oligonucleotides used to analyze gene expression by RT-PCR		
4100	CGTCGGATCGCGCCATAC	Forward primer to amplify *lipO*
4099	GCACCTTCGCGAGATGCC	Reverse primer to amplify *lipO*
4104	GCGCGATCGATCAGTGGTAC	Forward primer to amplify *lip2*
4103	GTCACCGATGCGACGAGTT	Reverse primer to amplify *lip2*

774